A Mathematical Theory of Historical Greenhouse Gas Emissions with Rigorous Insights

Rizal Purnawan[*]

[*]Independent Researcher, East Jakarta, 13760, DKI Jakarta, Indonesia.

[*]Corresponding author. E-mail: rizalpurnawan23@gmail.com; ORCID: 0000-0001-8858-4036

Abstract

In this paper, we analyze historical greenhouse gas (GHG) emissions worldwide, leveraging a dataset provided by (Gütschow and Pflüger, 2023). Employing mathematical modeling, a formal theory is developed, describing the growth trajectories of GHG emissions over time. The theory introduces several key concepts including continuous emission process (CEP), discrete emission process (DEP), historical upper bound emission (HUBE), historical peak emission (HPE), rapid growing emission (RGE), rapid shrinking emission (RSE), pivotal periods (piviods), historical expected growth rate (HEGR) and conditional historical bound space (CHBS), pinpointing important periods and numerical measures related to a country's GHG emission growth. A notable invention in the theory is the concept of piviods developed from the concept of Lipschitz continuity and short map in mathematical analysis, highlighting a country's transition from slow to rapid GHG emission growth and vice versa. Additionally, machine learning algorithms and computer algebra systems are also utilized in the computational implementation of the theory, enhancing the robustness and efficiency. Our findings reveal valuable insights into historical GHG emissions, offering a novel approach to their analysis and bridging the gap between formal mathematics and environmental science.

Keywords: Greenhouse Gas Emissions, Environmental Science, Formal Theory, Mathematical Analysis, Machine Learning, Computer Algebra System

1   Introduction

One of the key physical factors supporting life on Earth is the greenhouse effect (GHE) within Eart's atmosphere. The sun emits shortwave radiation as a result of nuclear fusion reactions at its core, which travels through space and reaches Eart. Some of this radiation is reflected by Eart's atmosphere, while the rest is absorbed. The absorbed shortwave radiation easily penetrates Eart's atmosphere and reaches Eart's surface, providing essential energy for life. However, the received radiation is subsequently re-emitted back into space by Eart in the form of longwave radiation. As this re-emission travels outward, some of the radiation is trapped and absorbed by greenhouse gases (GHGs), which is then re-emitted back into Eart's atmosphere, warming both the atmosphere and Eart's surface. This phenomenon is known as the greenhouse effect (GHE) (Treut et al., 2007). Without the greenhouse effect, Eart's average temperature would be much colder (Treut et al., 2007), rendering it inhospitable for most life forms on the planet. A notable example of a severe greenhouse effect is the atmosphere of planet Venus.

Among the gases classified as GHGs are carbon dioxide (CO_2), methane (CH_4), nitrous oxide (N_2O), nitrogen trifluoride (NF_3), and sulfur hexafluoride (SF_6) (Treut et al., 2007). Carbon dioxide CO_2 is a naturally occurring gas and an essential component of Earth's atmosphere, released and absorbed through natural processes such as respiration (Patel et al., 2022), photosynthesis, and volcanic activity. Methane (CH_4) is also naturally occurring, produced by various processes, including the decay of organic matter in anaerobic conditions and the digestive processes of certain microbes and animals (Thiel, 2018). Nitrous oxide (N_2O), another naturally occurring GHG, is produced by both natural and human-related activities, including microbial processes in soils and oceans (Sloss, 1992) and combustion processes. In contrast, nitrogen trifluoride (NF_3) (Henderson and Woytek, 2000) and sulfur hexafluoride (SF_6) (Dervos and Vassilou, 2000) are synthetic GHGs, manufactured through industrial processes and not naturally occurring in Eart's atmosphere. They are produced for specific industrial purposes (Henderson and Woytek, 2000; Dervos and Vassilou, 2000).

The primary issue today is the substantial increase in greenhouse gas (GHG) concentrations in Eart's atmosphere, driven by industrialization and various human activities (Treut et al., 2007). This surge has led to a phenomenon known as global warming (GW), characterized by a significant rise in surface temperatures (Treut et al., 2007). The consequences of global warming are far-reaching, encompassing extreme changes in Earth's climate, alterations in precipitation patterns, the proliferation of more frequent and severe heatwaves, and an increase in the average sea level due to the melting of polar ice (Treut et al., 2007). These impacts have resulted in disasters at various locations around the world, posing imminent dangers to life forms on Earth.

Addressing the greenhouse effect (GHE) to prevent catastrophic outcomes begins with the maintenance of greenhouse gas (GHG) concentrations in Eart's atmosphere. While this undertaking proves to be challenging, the potential threats to life on Earth escalate without proactive efforts to stabilize the GHE. Exploring insights derived from historical data on GHG emissions is integral to these efforts, offering a potentially more effective approach to the case.

Insights such as the periods in which a country reached the historical maximum concentration of GHE, or experienced the highest growth rate of GHE, or started to produce exponential GHE, and the historical growth rate of GHE are important information which would help the efforts in maintaining GHG concentrations. These information could be integrated with historical activities of countries to figure out the accurate causes of exponential growth of emissions.

The main question to be answered by this paper is the rigorous method in determining these insights from the historical dataset of GHG emissions. Therefore, we develop a rigorous mathematical theory to answer this question. The dataset which will become the basis of the investigation is the GHE dataset provided by (Gütschow and Pflüger, 2023).

2   Overview of Datasets: GHGs Emissions

In this paper, we leverage a GHGs emissions dataset obtained from (Gütschow and Pflüger, 2023) with the methodology provided by (Gütschow et al., 2016). Our preprocessing involved meticulous steps, including data cleansing to address missing values, such as certain early years

lacked records of GHGs concentrations for specific countries. We also conducted feature selection to retain only the essential features in the post-processing phase. The Pyhon library Pandas (pandas development team, 2020) is incorporated in the data preprocessing and the Python library Matplotlib (Hunter, 2007) is employed for data visualization.
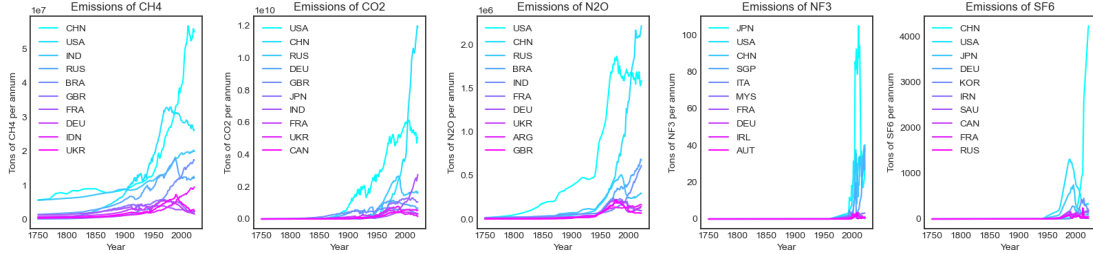

Figure 1: Top ten countries with emissions

Figure 1 illustrates the plots of top ten countries by the total GHG emissions, plotted based on types of GHG. The data shows that China, USA, India, Russia, Brazil, Great Britain, France, Germany, Indonesia and Ukraine are top ten countries with largest total emissions of methane (CH_4). The countries USA, China, Russia, Germany, Great Britain, Japan, India, France, Ukraine and Canada are the top ten total emitters of carbon dioxide (CO_2). The countries USA, China, Russia, Brazil, India, France, Germany, Ukraine, Argentina and Great Britain are the top ten total emitters of nitrous oxide (N_2O). The countries Japan, USA, China, Singapore, Italy, Malaysia, France, Germany, Ireland and Austria are the top ten total emitters of nitrogen trifluoride (NF_3). Then the countries China, USA, Japan, Germany, South Korea, Iran, Saudi Arabia, Canada, France and Russia are the top ten total emitters of ulfur hexafluoride (SF_6). The consistent countries sitting on the top ten of total emitters of all these GHGs include USA, China, France and Germany. We will dig deeper insights related to GHG emissions on subsequent sections.

3 Mathematical Framework and Algorithms

The aim of this research is exploring the historical dataset (Gütschow and Pflüger, 2023) of GHGs emissions to gain insights. A systematic approach to this aim is by modelling the dataset into a formal mathematical language. It would be much more convenient if we can express the historical GHGs concentrations as deterministic functions with respect to time, moreover, if such functions are continuously differentiable. With this property, we can analyse the rate of change of GHGs concentrations in a nicer manner by applying machinery of real analysis (Rudin, 1964). The rate of change will represent the growth of the GHGs emissions over time. This approach will also help us identify pivotal years of countries experiencing exponential growths of GHEs.

First, we will develop a formal mathematical model related to the dataset (Gütschow and Pflüger, 2023) and its structure by incorporating probability theory (Brémaud, 2020), measure theory (Salamon, 2016), functional analysis (Kreyszig, 1978) and topology (André, 2020). In particular, we will express the functions representing time-dependent GHGs concentrations as a stochastic process (Brémaud, 2020). In addition, set theory (Brémaud, 2020) and first-order logic (Bergmann et al., 2014) will be employed regularly as the formal language in the discussion.

3.1 Probability Theoretic Model of Historical Emissions

The records presented in the GHG emissons dataset (Gütschow and Pflüger, 2023) are yearly GHGs concentrations as illustrated in figure 1, hence we have a discrete data. In our approach, we will construct continuous functions representing the data in a time-dependent manner. For a generality, suppose $y_0, y_e \in \mathbb{N}$ with $0 < y_0 < y_e < \infty$ such that y_0 represents the year of the

first record in the dataset and y_e represents the year of the latest record in the dataset. Let

$$T := [y_0, y_e] \subset \mathbb{R} \tag{1}$$

be the set (Stoll, 1963) representing the compact (André, 2020) time interval between the end points of time in the dataset. Then a set

$$\tilde{T} := \{t \in T \mid \exists k \in \mathbb{N}_0[t = y_0 + k \le y_e]\} \tag{2}$$

where $\mathbb{N}_0 := \{0, 1, 2, \dots\}$, is the time points in the dataset (Gütschow and Pflüger, 2023). This generality is intended to maintain the validity of the theory even if the dataset (Gütschow and Pflüger, 2023) is periodically updated.

Note that there are two more components in the dataset (Gütschow and Pflüger, 2023), namely the countries and the types of GHG. Let C be a set representing the countries in the dataset and let G be a set representing the types of GHG in the dataset.

Suppose a probability space (Brémaud, 2020) $(CG, \mathcal{C}, P)$ such that

$$CG := C \times G, \tag{3}$$

$\mathcal{P}(CG) \supseteq \mathcal{C}$ is a σ-algebra (Salamon, 2016) representing the event space on CG and $P : \mathcal{C} \to [0, 1]$ is a probability measure (Brémaud, 2020; Salamon, 2016). In the dataset (Gütschow and Pflüger, 2023), we have a real-valued stochastic process (Brémaud, 2020) $\{\tilde{X}_t\}_{t \in \tilde{T}}$ with respect to $(CG, \mathcal{C}, P)$ such that $\tilde{X}_t(c, g)$ is the concentration of a GHG of type $g \in G$ in a country $c \in C$ at a time $t \in \tilde{T}$. It is worth emphasizing that the value of $\tilde{X}_t(c, g)$ is in the dataset (Gütschow and Pflüger, 2023), for any $c \in C$, $g \in G$ and $t \in \tilde{T}$. On the other hand, what we are about to construct is another real-valued stochastic process $\{X_t\}_{t \in T}$ which is a continuous approximation to $\{\tilde{X}_t\}_{t \in \tilde{T}}$. For the discussion in this paper, let us refer $\{\tilde{X}_t\}_{t \in \tilde{T}}$ to as the discrete emission process (DEP) and $\{X_t\}_{t \in T}$ to as the continuous emission process (CEP). To shape the CEP $\{X_t\}_{t \in T}$, we propose the following postulate.

Postulate 1. The CEP, stochastic process $\{X_t\}_{t \in T}$ with respect to $(CG, \mathcal{C}, P)$, satisfies the following properties:

P1 The CEP is bounded everywhere, i. e.,

$$\forall t \in T \forall c \in C \forall g \in G : \ |X_t(c, g)| < \infty \,.$$

P2 The CEP $\{\tilde{X}_t\}_{t \in \tilde{T}}$ has well-defined first 3 continuous partial derivatives at every point in the interior of T, that is,

$$\forall t \in \text{int}(T) \forall c \in C \forall g \in G \forall k \in \{1, 2, 3\} \exists L \in \mathbb{R} : \ \frac{\partial^k}{\partial t^k} X_t(c, g) = L \,,$$

where $\text{int} : \mathcal{P}(\mathbb{R}) \to \mathcal{T}_{\mathbb{R}}$ is the interior operator on the standard Euclidean topological space $(\mathbb{R}, \mathcal{T}_{\mathbb{R}})$ (André, 2020).

3.2 Properties of Discrete and Continuous Emission Processes

Both the DEP $\{\tilde{X}_t\}_{t \in \tilde{T}}$ and the CEP $\{X_t\}_{t \in T}$ can be realized into multivariable functions

$$\tilde{X} : \tilde{T} \times C \times G \to \mathbb{R} \quad \text{and} \quad X : T \times C \times G \to \mathbb{R} \tag{4}$$

respectively. And we have

$$\forall t \in \tilde{T} \forall c \in C \forall g \in G : \ \tilde{X}(t, c, g) = \tilde{X}_t(c, g)$$

for the DEP, and

$$\forall t \in T \forall c \in C \forall g \in G : \ X(t, c, g) = X_t(c, g)$$

for the CEP. These realizations will be convenient for a systematic construction of the CEP.

Now we will construct some measure spaces to which the realizations of the DEP and the CEP are belonging. Let $(\tilde{T}, \tilde{\mathcal{A}}, \alpha)$ and $(T, \mathcal{A}, \lambda)$ be measure spaces (Salamon, 2016) on $\tilde{T}$ and T respectively such that $\alpha : \tilde{\mathcal{A}} \to \mathbb{N}$ is a counting measure (Salamon, 2016) on $(\tilde{T}, \tilde{\mathcal{A}})$ and $\lambda : \mathcal{A} \to [0, \infty]$ is a Lebesgue measure (Salamon, 2016) on $(T, \mathcal{A})$. In particular, $\tilde{\mathcal{A}}$ is designated to be the power set (Stoll, 1963) of $\tilde{T}$, that is, $\tilde{\mathcal{A}} := \mathcal{P}(\tilde{T})$. We will present some measure theoretic properties of the DEP and the CEP with respect to $(\tilde{T}, \tilde{\mathcal{A}}, \alpha)$ and $(T, \mathcal{A}, \lambda)$ respectively. However, let us first observe a notion in measure theory which relates to the properties of the DEP and the CEP.

Definition 1 (L^p Space)**.** Suppose a measure space $(S, \mathcal{S}, \mu)$ (Salamon, 2016). Let $p \in [1, \infty)$. A vector space (Roman, 2005) denoted by $L^p(\mu)$ is a vector space of Lebesgue p-integrable functions (Salamon, 2016). A measurable function $f : S \to \mathbb{R}$ has a property $f \in L^p(\mu)$ if and only if

$$\left(\int_S |f|^p \, \mathrm{d}\mu \right)^{\frac{1}{p}} < \infty$$

holds.

Another measure theoretic notion related to L^p-space and the DEP as well as the CEP is the integrability of bounded everywhere measurable functions. This notion is formally presented in the following theorem.

Theorem 1. *Let $(S, \mathcal{S}, \mu)$ be a measure space. Let $p \in [1, \infty)$. And let $f : S \to \mathbb{R}$ be a measurable function. The statement*

$$\forall x \in S \big[|f(x)| < \infty \big] \; \wedge \; \mu(S) < \infty \implies f \in L^p(\mu)$$

holds.

Proof. Note that

$$\int_S |g| \, \mathrm{d}\mu \leq \mu(S) \cdot \sup_{x \in S} |g(x)|$$

holds for every measurable function $g : S \to \mathbb{R}$. Now suppose

$$\forall x \in S \big[|f(x)| < \infty \big]$$

and $\mu(S) < \infty$ are true. Then there exists some $B \in (0, \infty)$ such that

$$\forall x \in S : \; |f(x)| \leq B \,.$$

It follows that

$$\sup_{x \in S} |g(x)| \leq B \,.$$

Then we obtain

$$\int_S |f|^p \, \mathrm{d}\mu \leq \mu(S) \cdot B^p \,,$$

which implies

$$\left(\int_S |f|^p \, \mathrm{d}\mu \right)^{\frac{1}{p}} \leq \sqrt[p]{\mu(S)} \cdot B < \infty \,.$$

And follows from definition 1, the result above shows that $f \in L^p(\mu)$. $\qquad \square$

Let us now observe the very first measure theoretic property related to the DEP and the CEP in the following lemma.

Lemma 1. *The measures $\alpha : \tilde{\mathcal{A}} \to \mathbb{N}$ on $(\tilde{T}, \tilde{\mathcal{A}})$ and $\lambda : \mathcal{A} \to [0, \infty]$ are finite measures (Salamon, 2016).*

Proof. Since α by our definition is a counting measure (Salamon, 2016), meaning that

$$\forall A \in \tilde{\mathcal{A}} : \ \alpha(A) = |A| \,,$$

then we obtain

$$\alpha(\tilde{T}) = |\tilde{T}| = y_e - (y_0 - 1) = y_e - y_0 + 1 < \infty \,,$$

as there are only finitely many data points in the dataset (Gütschow and Pflüger, 2023). Thus, α is a finite measure on $(\tilde{T}, \tilde{\mathcal{A}})$.

On the other hand, as designated, $\lambda : \mathcal{A} \to [0, \infty]$ is a Lebesgue measure (Salamon, 2016). Suppose $A \in \mathcal{A}$ such that there exists some $\{A_i\}_{i \in I}$ with

$$A = \bigcup_{i \in I} A_i \,,$$

where I is some countable index set, and $A_1, A_2, \ldots \in \mathcal{A}$ are intervals on $\mathbb{R}$ (Rudin, 1964). Then we have

$$\lambda(A) \le \sum_{i \in I} \lambda(A_i) = \sum_{i \in I} \sup A_i - \inf A_i \,.$$

Follows from a property of measure (Salamon, 2016), we have

$$\forall B, B' \in \mathcal{A} : \ \lambda(B) \le \lambda(B') \iff B \subseteq B' \,.$$

And we will always have

$$\forall B \in \mathcal{A} : \ \lambda(B) \le \lambda(T)$$

since

$$\forall B \in \mathcal{A} : \ B \subseteq T \,.$$

Then we obtain

$$\forall B \in \mathcal{A} : \ \lambda(B) \le \lambda(T) = \sup T - \inf T = y_e - y_0 < \infty \,,$$

which shows that λ is a finite measure on $(T, \mathcal{A})$. $\qquad\square$

Theorem 1 and lemma 1 are crucial for another measure theoretic property which directly belongs to the DEP and the CEP respectively. In fact, they form bases for the proof of the property which is presented in the following theorem.

Theorem 2. *Let us fix a point $(c, g) \in C \times G$. Suppose some maps*

$$\tilde{X}_{c,g} := \tilde{X}\big|_{\tilde{T} \times \{(c,g)\} \subset \tilde{T} \times C \times G} : \tilde{T} \to \mathbb{R}$$

and

$$X_{c,g} := X\big|_{T \times \{(c,g)\} \subset T \times C \times G} : T \to \mathbb{R}$$

such that

$$\forall t \in \tilde{T} : \ \tilde{X}_{c,g}(t) = \tilde{X}(t, c, g)$$

$$\forall t \in T : \ X_{c,g}(t) = X(t, c, g)$$

hold. Then the following properties also hold: (i) $\tilde{X} \in L^2(\alpha)$; (ii) $X \in L^2(\lambda)$.

Proof. First, we prove property (i). As designated earlier, $\tilde{\mathcal{A}}$ is the power set of $\tilde{T}$, hence, every subset of $\tilde{T}$ is a measurable set (Salamon, 2016). It guarantees that $X_{c,g}$ is $\tilde{\mathcal{A}}$-measurable (Salamon, 2016). Note that the values of $\{\tilde{X}_t\}_{t \in \tilde{T}}$ in the dataset (Gütschow and Pflüger, 2023) are all finite. Consequently,

$$\forall t \in \tilde{T} : \ |\tilde{X}_{c,g}(t)| < \infty \,,$$

meaning that $X_{c,g}$ is bounded everywhere. Lemma 1 asserts that α is a finite measure on $(\tilde{T}, \tilde{\mathcal{A}})$. Hence, by theorem 1, $X_{c,g} \in L^2(\alpha)$.

Now we prove property (ii). Postulate P2 asserts the existence of partial derivative of $X_t(c,g)$ with respect to t, for every $t \in T$. In other words, $X_{c,g}$ is differentiable. Since differentiability implies continuity (Rudin, 1964), then $X_{c,g}$ is a continuous function. As every continuous function is measurable (Salamon, 2016), then $X_{c,g}$ is $\mathcal{A}$-measurable function. Then by postulate P1, $X_{c,g}$ is bounded everywhere. Lemma 1 asserts that λ is a finite measure on $(T, \mathcal{A})$. Hence, by theorem 1, $X_{c,g} \in L^2(\lambda)$. $\qquad\square$

Lemma 1 asserts the finiteness of measures α and λ. While theorem 2 asserts that both the DEP and the CEP are Lebesgue square-integrable functions (Salamon, 2016) with respect to their measure spaces. These measure theoretic properties will be essential in the subsequent formulation of the DEP and the CEP in terms of probability theory. Another observation is provided in the following proposition.

Proposition 1. Let us fix a point $(c,g) \in C \times G$. A restriction $X_{c,g}|_{\tilde{T}} : \tilde{T} \to \mathbb{R}$ defined by

$$\forall t \in \tilde{T} : \ X_{c,g}|_{\tilde{T}}(t) = X_{c,g}(t)$$

has a property $X_{c,g}|_{\tilde{T}} \in L^2(\alpha)$. It follows from the fact that $\tilde{\mathcal{A}}$ is the power set of $\tilde{T}$, implying that $X_{c,g}|_{\tilde{T}}$ is measurable, $X_{c,g}|_{\tilde{T}}$ is bounded everywhere since $X_{c,g}$ is bounded everywhere and that α is a finite measure on $(\tilde{T}, \tilde{\mathcal{A}})$ and a consequence of theorem 1.

Let us refer $X_{c,g}|_{\tilde{T}}$ in proposition 1 to as the approximate discrete emission process (ADEP). Now we introduce some maps $P_\alpha : \tilde{\mathcal{A}} \to [0,1]$ and $P_\lambda : \mathcal{A} \to [0,1]$ defined by

$$\forall A \in \tilde{\mathcal{A}} : \ P_\alpha(A) := \frac{\alpha(A)}{\alpha(\tilde{T})} \tag{5}$$

and

$$\forall A \in \mathcal{A} : \ P_\lambda(A) := \frac{\lambda(A)}{\lambda(T)} \tag{6}$$

respectively.

We will present the first property related to P_α and P_λ in the form of a theorem. However, we will first present the formal definition of probability measure and probability space (Salamon, 2016), since this definition will be a basis for the theorem.

Definition 2 (Probability Space). A probability measure (Brémaud, 2020) on a measurable space $(\Omega, \mathcal{F})$ (Salamon, 2016) is a map $P : \mathcal{F} \to [0,1]$ which satisfies the following axioms (Brémaud, 2020):

K1 $\forall A \in \mathcal{F} : \ P(A) \geq 0$

K2 $P(\Omega) = 1$

K3 If $\{A_k\}_{k=1}^\infty \subseteq \mathcal{F}$ such that

$$\forall i, j \in \mathbb{N} : \ i \neq j \implies A_i \cap A_j = \varnothing \,,$$

then

$$P\left(\bigcup_{k=1}^\infty A_k\right) = \sum_{k=1}^\infty P(A_k) \,.$$

The first probability theoretic property of P_α and P_λ is the fact that the two are probability measures. This statement is formally presented in the following theorem.

Theorem 3. *(i) The map $P_\alpha : \tilde{\mathcal{A}} \to [0,1]$ is a probability measure on measurable space $(\tilde{T}, \tilde{\mathcal{A}})$. (ii) The map $P_\lambda : \mathcal{A} \to [0,1]$ is also a probability measure on measurable space $(T, \mathcal{A})$.*

Proof. (i) Note that α is nonnegative, then it can be guaranteed that P_α satisfies axiom K1. From the definition of P_α, we obtain

$$P_\alpha(\tilde{T}) = \frac{\alpha(\tilde{T})}{\alpha(\tilde{T})} = 1\,,$$

and hence P_α satisfies axiom K2. Axiom K3 is also an axiom of measure (Salamon, 2016), hence α satisfies this axiom as well. Let $\{A_k\}_{k=1}^\infty \subseteq \tilde{\mathcal{A}}$ such that

$$\forall i,j \in \mathbb{N}: \; i \neq j \implies A_i \cap A_j = \varnothing\,.$$

Then we obtain

$$P_\alpha\left(\bigcup_{k=1}^\infty A_k\right) = \frac{1}{\alpha(\tilde{T})}\alpha\left(\bigcup_{k=1}^\infty A_k\right) = \frac{1}{\alpha(\tilde{T})}\sum_{k=1}^\infty \alpha(A_k) = \sum_{k=1}^\infty \frac{\alpha(A_k)}{\alpha(\tilde{T})} = \sum_{k=1}^\infty P_\alpha(A_k)\,,$$

which shows that P_α also satisfies axiom K3. Hence P_α is a probability measure on $(\tilde{T}, \tilde{\mathcal{A}})$ by definition 2.

(ii) Measure λ is also nonnegative, then it can be guaranteed that P_λ satisfies axiom K1. From the definition of P_λ, we obtain

$$P_\lambda(T) = \frac{\lambda(T)}{\lambda(T)} = 1\,,$$

and hence P_λ satisfies axiom K2. Likewise, as axiom K3 is also an axiom of measure, λ satisfies axiom K3. Let $\{B_k\}_{k=1}^\infty \subseteq \mathcal{A}$ such that

$$\forall i,j \in \mathbb{N}: \; i \neq j \implies B_i \cap B_j = \varnothing\,.$$

Then we obtain

$$P_\lambda\left(\bigcup_{k=1}^\infty B_k\right) = \frac{1}{\lambda(T)}\lambda\left(\bigcup_{k=1}^\infty B_k\right) = \frac{1}{\lambda(T)}\sum_{k=1}^\infty \lambda(B_k) = \sum_{k=1}^\infty \frac{\lambda(B_k)}{\lambda(T)} = \sum_{k=1}^\infty P_\lambda(B_k)\,,$$

which shows that P_λ also satisfies axiom K3. Hence P_λ is a probability measure on $(T, \mathcal{A})$ by definition 2. $\qquad\square$

In addition to theorem 3, $(\tilde{T}, \tilde{\mathcal{A}}, P_\alpha)$ and $(T, \mathcal{A}, P_\lambda)$ are probability spaces (Brémaud, 2020) by definition 2. Another property of P_α and P_λ is presented in the following proposition.

Proposition 2. Follows from the definition of P_α and P_λ, we obtain

$$\forall A \in \tilde{\mathcal{A}}: \; P_\alpha(A) = \frac{\alpha(A)}{\alpha(\tilde{T})} \leq \alpha(A)$$

and

$$\forall A \in \mathcal{A}: \; P_\lambda(A) = \frac{\lambda(A)}{\lambda(T)} \leq \lambda(A)\,.$$

Hence it can be inferred that

$$\forall A \in \tilde{\mathcal{A}}: \; \alpha(A) = 0 \implies P_\alpha(A) = 0$$

and

$$\forall A \in \mathcal{A}: \; \lambda(A) = 0 \implies P_\lambda(A) = 0$$

showing that $P_\alpha \ll \alpha$ (P_α is absolutely continuous with respect to α) and $P_\lambda \ll \lambda$ (P_λ is absolutely continuous with respect to λ) (Salamon, 2016). In this setting, $\frac{1}{\alpha(\tilde{T})}$ is the Radon-Nikodým derivative (Salamon, 2016) of P_α, that is,

$$\frac{1}{\alpha(\tilde{T})} = \frac{\mathrm{d}P_\alpha}{\mathrm{d}\alpha}\,,$$

and $\frac{1}{\lambda(T)}$ is the Radon-Nikodỳm derivative (Salamon, 2016) of λ, that is,

$$\frac{1}{\lambda(T)} = \frac{\mathrm{d}P_\lambda}{\mathrm{d}\lambda}.$$

In theorem 2 and proposition 1, we have shown that the DEP, the CEP and the ADEP are Lebesgue square-integrable functions. It is interesting to observe whether the similar property holds in terms of probability spaces $(\tilde{T}, \tilde{\mathcal{A}}, P_\alpha)$ for the DEP as well as the ADEP, and $(T, \mathcal{A}, P_\lambda)$ for the CEP. The formal observation to this possible property is presented in the following theorem.

Theorem 4. *Let us fix a point $(c, g) \in C \times G$. The following properties hold:*

i. $\tilde{X}_{c,g} \in L^2(P_\alpha)$

ii. $X_{c,g} \in L^2(P_\lambda)$

iii. $X_{c,g}|_{\tilde{T}} \in L^2(P_\alpha)$

Proof. We will prove the properties in this theorem simultaneously. Note that

$$\left(\int_{\tilde{T}} \tilde{X}_{c,g}^2 \, \mathrm{d}\alpha \right)^{\frac{1}{2}}, \ \left(\int_T X_{c,g}^2 \, \mathrm{d}\lambda \right)^{\frac{1}{2}}, \ \left(\int_{\tilde{T}} \left(X_{c,g}|_{\tilde{T}} \right)^2 \mathrm{d}\alpha \right)^{\frac{1}{2}} < \infty$$

holds by theorem 2 and proposition 1. Then by the Radon-Nikodým properties of P_α and P_λ, we obtain

$$\left(\int_{\tilde{T}} \tilde{X}_{c,g}^2 \, \mathrm{d}P_\alpha \right)^{\frac{1}{2}} = \left(\int_{\tilde{T}} \tilde{X}_{c,g}^2 \frac{\mathrm{d}P_\alpha}{\mathrm{d}\alpha} \, \mathrm{d}\alpha \right)^{\frac{1}{2}} = \left(\frac{1}{\alpha(\tilde{T})} \int_{\tilde{T}} \tilde{X}_{c,g}^2 \, \mathrm{d}\alpha \right)^{\frac{1}{2}} \leq \left(\int_{\tilde{T}} \tilde{X}_{c,g}^2 \, \mathrm{d}\alpha \right)^{\frac{1}{2}} < \infty$$

which proves property (i),

$$\left(\int_T X_{c,g}^2 \, \mathrm{d}P_\lambda \right)^{\frac{1}{2}} = \left(\int_T X_{c,g}^2 \frac{\mathrm{d}P_\lambda}{\mathrm{d}\lambda} \, \mathrm{d}\lambda \right)^{\frac{1}{2}} = \left(\frac{1}{\lambda(T)} \int_T X_{c,g}^2 \, \mathrm{d}\lambda \right)^{\frac{1}{2}} \leq \left(\int_T X_{c,g}^2 \, \mathrm{d}\lambda \right)^{\frac{1}{2}} < \infty$$

which proves property (ii), and

$$\begin{aligned}
\left(\int_{\tilde{T}} \left(X_{c,g}|_{\tilde{T}} \right)^2 \mathrm{d}P_\alpha \right)^{\frac{1}{2}} &= \left(\int_{\tilde{T}} \left(X_{c,g}|_{\tilde{T}} \right)^2 \frac{\mathrm{d}P_\alpha}{\mathrm{d}\alpha} \, \mathrm{d}\alpha \right)^{\frac{1}{2}} \\
&= \left(\frac{1}{\alpha(\tilde{T})} \int_{\tilde{T}} \left(X_{c,g}|_{\tilde{T}} \right)^2 \mathrm{d}\alpha \right)^{\frac{1}{2}} \\
&\leq \left(\int_{\tilde{T}} \left(X_{c,g}|_{\tilde{T}} \right)^2 \mathrm{d}\alpha \right)^{\frac{1}{2}} \\
&< \infty
\end{aligned}$$

which proves property (iii). Hence the theorem is proven. $\square$

In fact, the proof of theorem 4 can also be given from the facts that P_α and P_λ are finite measures, the DEP, the CEP and the ADEP are bounded everywhere, and consequently the DEP, the CEP and the ADEP are Lebesgue square-integrable functions with respect to their probability spaces by theorem 1.

Theorem 4 implies that probability theoretic operations are well-defined on the DEP, the CEP and the ADEP, including expectation, conditional expectation, covariance, variance, conditional variance, standard deviation, conditional standard deviation and correlation (Brémaud, 2020) with respect to probability space $(\tilde{T}, \tilde{\mathcal{A}}, P_\alpha)$ for the DEP as well as the ADEP, and probability space $(T, \mathcal{A}, P_\lambda)$ for the CEP. This result is crucial in the construction of the CEP.

3.3 Construction of the Continuous Emission Process

An approach we take to construct the CEP is by making use of polynomial functions with respect to the time. The type of polynomial function that we use will be Bernstein polynomial (Lorentz, 2012), which offers a considerable accuracy and robustness. The formal definition of Bernstein polynomial (Lorentz, 2012) is presented as follows.

Definition 3 (Bernstein Polynomial). Let $n \in \mathbb{N}$. A Bernstein polynomial is a map $f : \mathbb{R} \to \mathbb{R}$ defined by

$$\forall x \in U : \ f(x) := \sum_{k=0}^{n} \binom{n}{k} \beta_{k,n} x^k (1-x)^{n-k} \, ,$$

where $\beta_{0,n}, \beta_{1,n}, \ldots, \beta_{n,n} \in \mathbb{R}$ with $\beta_{n,n} \neq 0$ are unknown constants and $\binom{n}{k}$ is the binomial coefficient of the the k-term, for every $k \in \{0, 1, \ldots, n\}$.

The nice property of Bernstein polynomials is the smoothness property (Lorentz, 2012), which implies 3-times differentiability (Rudin, 1964) of the polynomial. This property is consistent with axiom P2 of postulate 1. Hence, we define the CEP by

$$\forall c \in C \forall g \in G \forall t \in T : \ X_{c,g}(t) := \sum_{k=0}^{p} \binom{p}{k} \beta_{c,g,k} t^k (1-x)^{p-k} \tag{7}$$

where $\beta_{c,g,0}, \beta_{c,g,1}, \ldots, \beta_{c,g,p} \in \mathbb{R}$ are unknown constants with $\beta_{c,g,p} \neq 0$ and some $p \in \mathbb{N}$. Now we need to establish the necessary condition for the CEP, which will be presented as a postulate. However, we will need to construct some topology on $\tilde{T}$. First, let us observe the following definition.

Definition 4 (Open Ball Operator). Suppose a metric space (S, d) (André, 2020). Let $(S, \mathcal{T})$ be a metrizable space (André, 2020) with respect to (S, d). Let $\rho > 0$. An open ball operator of radius ρ is a map $B_\rho : S \to \mathcal{T}$ defined by

$$\forall x \in S : \ B_\rho(x) := \{u \in S \mid d(u, x) < \rho\} \, .$$

And we call the set $B_\rho(s)$ an open ball of radius ρ centered at s, for any point $s \in S$.

Suppose a metric space $(\tilde{T}, \tilde{d})$ (André, 2020) such that the metric (André, 2020) $\tilde{d} : \tilde{T} \times \tilde{T} \to \mathbb{R}$ is defined by

$$\forall t, u \in \tilde{T} : \ \tilde{d}(t, u) := |t - u| \, . \tag{8}$$

Note that $\tilde{d} : \tilde{T} \times \tilde{T} \to \mathbb{R}$ as defined in expression 8 is a valid metric (André, 2020). Now let $(\tilde{T}, \tilde{\mathcal{T}})$ be a metrizable space with respect to $(\tilde{T}, \tilde{d})$ (André, 2020). The fundamental property of $(\tilde{T}, \tilde{\mathcal{T}})$ is presented in the following theorem.

Theorem 5. *Topological space $(\tilde{T}, \tilde{\mathcal{T}})$ is in fact a discrete topology (André, 2020).*

Proof. A topology is called discrete topology if it contains every subset of the underlying set (André, 2020). In other words, a discrete topology is equal to the power set. To prove this theorem, we need to show that every subset of $\tilde{T}$ is open (i. e., an element of $\tilde{\mathcal{T}}$). Every topology contains the empty set and the underlying set of the space (André, 2020), implying that $\varnothing, \tilde{T} \in \tilde{\mathcal{T}}$. Then, it is left to show that every nonempty subset of $\tilde{T}$ is open. And a set is open in a metrizable space if and only it can be expressed as the union of open balls each centred at each point in the set (André, 2020).

Let $A \subset \tilde{T}$ such that $A \neq \varnothing$. Then, A must contains some points. As defined in expression 2, $\tilde{T}$ are integers in between 1750 and 2022 inclusive. Let $\rho \in \mathbb{R}$ such that $0 < \rho < 1$. And we have

$$\forall a \in A : \ B_\rho(a) = \{t \in \tilde{T} \mid \tilde{d}(t, a) < \rho\} = \{t \in \tilde{T} \mid |t - a| < \rho\} = \{a\} \, .$$

Then we obtain

$$\bigcup_{a \in A} B_\rho(a) = \bigcup_{a \in A} \{a\} = A \, ,$$

which shows that $A \in \tilde{\mathcal{T}}$. Once again, this property holds for every $A \subset T$ with $A \neq \varnothing$. Hence, every subset of $\tilde{T}$ is an element of $\tilde{\mathcal{T}}$. Consequently, $\tilde{\mathcal{T}}$ is a discrete topology on $\tilde{T}$. □

The following proposition follows directly from theorem 5.

Proposition 3. Follows from theorem 5, we have that $\tilde{\mathcal{A}} = \tilde{\mathcal{T}}$. Hence $\tilde{\mathcal{A}}$ is the Borel σ-algebra with respect to $\tilde{\mathcal{T}}$ (Salamon, 2016). It implies that every open ball $B_\rho(t)$ is $\tilde{\mathcal{A}}$-measurable, for some $\rho > 0$ and for every $t \in \tilde{T}$.

The necessary condition for the CEP is presented in the following postulate.

Postulate 2. Let $c \in C$ and $g \in G$. Follows from theorem 4, we have that $\tilde{X}_{c,g}, X_{c,g}|_{\tilde{T}} \in L^2(P_\alpha)$. Suppose a map

$$\text{MA} : (0, \infty) \times L^2(P_\alpha) \to L^2(P_\alpha)$$

defined by

$$\forall w \in (0, \infty) \forall f \in L^2(\alpha) \forall t \in \tilde{T} : \ \text{MA}(w, f)(t) := \text{E}[f \mid B_w(t)],$$

where $\text{E}[\,\cdot\mid\cdot\,] : L^1(\alpha) \times \tilde{\mathcal{A}} \to \mathbb{R}$ is the conditional expectation operator (Brémaud, 2020) with respect to $(\tilde{T}, \tilde{\mathcal{A}}, P_\alpha)$. For some chosen $w \in (0, \infty)$, with the degree $p \in \mathbb{R}$ of the CEP Bernstein polynomial (Lorentz, 2012), there exists some considerably small $\rho > 0$ such that

$$\left\| \text{MA}(w, \tilde{X}_{c,g}) - X_{c,g}|_{\tilde{T}} \right\|_{2 : \text{MA}(w, \tilde{X}_{c,g}) - \text{E}[\text{MA}(w, \tilde{X}_{c,g})]}^2 \leq \rho$$

holds, where $\text{E} : L^1(P_\alpha) \to \mathbb{R}$ is the expectation operator (Brémaud, 2020), and $\|\cdot\|_{2:r} : L^2(P_\alpha) \to \mathbb{R}$ is the r-norm operator (Purnawan, 2023) with

$$r := \text{MA}(w, \tilde{X}_{c,g}) - \text{E}[\text{MA}(w, \tilde{X}_{c,g})]$$

in our case.

In a shorter language, the necessary condition for the CEP is that the ADEP shall be ρ-reliable with respect to the DEP (Purnawan, 2023), for some small $\rho > 0$. Note that the ADEP is in fact a restriction of the CEP on $\tilde{T}$. This condition will maintain the explainability of the CEP with respect to the dataset (Gütschow and Pflüger, 2023). And postulate 2 helps us find the best value of the polynomial degree p of the CEP given the value of w, which will be determined in practice.

3.4 Properties of the Continuous Emission Process

With the proposed postulates (postulate 1 and postulate 2) imposed on the CEP, historical insights regarding the GHGs and the GHEs can be inferred rigorously and systematically. In this section, we will present formal definitions regarding these historical insights.

The first property will be the time in which the historical maximum GHE occured in a country, which is a very natural observation. We will call such a time the "historical upper bound emission" (HUBE). The formal definition is presented as follows.

Definition 5 (Historical Upper Bound Emission)**.** Let $c \in C$ and $g \in G$. The time of historical upper bound emission (HUBE) of a country c of GHG g is a point $t_{ub} \in T$ such that

$$t_{ub} = \arg\max_{t \in T} X_{c,g}(t).$$

Note that $X_{c,g}$ is bounded everywhere by axiom P1. Hence, $X_{c,g}$ attains a global maximum (Rudin, 1964). Let $\rho > 0$. And the 2ρ-period of HUBE is an open ball $B_\rho(t_{ub})$.

It is always more convenient to make a reference to the period of HUBE than the time of HUBE, since the true time of HUBE might not be exactly at the one computed due to the fact that the polynomial approximation for the CEP with respect to the DEP is a smoothing process. Another property of the CEP closely related to HUBE is presented in the following definition.

Definition 6 (Historical Peak Emission)**.** Suppose a country $c \in C$ and a GHG $g \in G$. A point $t_p \in \text{int}(T)$ is called the time of historical peak emission (HPE) if and only if t_p is also the time of HUBE. Let $\rho > 0$. We call an open ball $B_\rho(t_p)$ the 2ρ-period of HPE if and only if $t_p \in \text{int}(T)$ is the time of HPE.

If we observe definitions 5 and 6, we can see that both the time and the period of HPE is both the time and the period of HUBE. In this sense, HPE is a stronger notion than HUBE. Also, the CEPs of some countries with some GHG types may not be equipped with HPE periods. Such a condition happens when either the emission in the country is still increasing or the emission in the country is decreasing from the first time of the record. Empirically, the former is most likely true than the latter. A very important property of HPE related to HUBE is presented in the following proposition.

Proposition 4. Suppose a country $c \in C$ and a GHG $g \in G$. Suppose $t_p \in \text{int}(T)$ is the time of HPE. By definition 6, t_p is also the time of HUBE. Then

$$\forall h > 0 : \ \frac{X(t_p + h, c, g) - X(t_p, c, g)}{h} \leq 0$$

and

$$\forall h < 0 : \ \frac{X(t_p + h, c, g) - X(t_p, c, g)}{h} \geq 0$$

necessarily hold. Then we obtain the limits

$$\frac{\partial}{\partial t_p^+} X(t_p, c, g) = \lim_{h \to 0^+} \frac{X(t_p + h, c, g) - X(t_p, c, g)}{h} \leq 0$$

and

$$\frac{\partial}{\partial t_p^-} X(t_p, c, g) = \lim_{h \to 0^-} \frac{X(t_p + h, c, g) - X(t_p, c, g)}{h} \geq 0 \, .$$

Note that $X_{c,g}$ is 3-times differentiable with respect to the time domain by axiom P2 of postulate 1. It implies that the limit shall exist and the right hand side and the left hand side limits above shall agree. Hence

$$\frac{\partial}{\partial t_p} X(t_p, c, g) = \frac{\partial}{\partial t_p^-} X(t_p, c, g) = \frac{\partial}{\partial t_p^+} X(t_p, c, g) = 0$$

holds.

Proposition 4 can be used to characterize the HPE of a CEP. The subsequent definition is regarding the period of rapid growing emission and the period of rapid shrinking emission. The formal definition is presented as follows.

Definition 7 (Periods of Rapid Growing and Shrinking Emissions)**.** Suppose a country $c \in C$ and a GHG $g \in G$. We define as follows:

i. A point $t_g \in \text{int}(T)$ is called the time of rapid growing emission (RGE) if and only if

$$T_g := \left\{ t \in \text{int}(T) \ \middle| \ \frac{\partial}{\partial t} X(t, c, g) > 0 \ \wedge \ \frac{\partial^2}{\partial t^2} X(t, c, g) = 0 \right\} \ \wedge \ T_g \neq \varnothing$$

and

$$t_g = \underset{t \in T_g}{\arg \sup} \ X(t, c, g)$$

holds.

ii. Let $\rho > 0$. We call an open ball $B_\rho(t_g)$ the 2ρ-period of RGE if and only if $t_g \in \text{int}(T)$ is the time of RGE.

iii. A point $t_s \in \text{int}(T)$ is called the time of rapid shrinking emission (RSE) if and only if

$$T_s := \left\{ t \in \text{int}(T) \; \middle| \; \frac{\partial}{\partial t} X(t, c, g) < 0 \; \wedge \; \frac{\partial^2}{\partial t^2} X(t, c, g) = 0 \right\} \; \wedge \; T_s \neq \varnothing$$

and

$$t_s = \underset{t \in T_s}{\arg \sup} \; X(t, c, g)$$

holds.

iv. Let $\rho > 0$. We call an open ball $B_\rho(t_s)$ the 2ρ-period of RSE if and only if $t_s \in \text{int}(T)$ is the time of RSE.

Note that both RGE and RSE may not exist for some country and GHG type. If both do exist, it is not always the case that the time of RGE is less than the time of RSE according to the theory we have developed. However, emipirically it may be the case. An important relation of HPE with both RGE and RSE is presented in the following theorem.

Theorem 6. *Suppose some country $c \in C$ and some GHG $g \in G$. Suppose both RGE and RSE exist for $X_{c,g}$. Let $B_{\rho_g}(t_g)$ and $B_{\rho_s}(t_s)$ be the $2\rho_g$-period of RGE and the $2\rho_s$-period of RSE respectively such that $t_g < t_s$. Then the period of HPE exists and*

$$t_g < t_p < t_s$$

holds where $t_p \in \text{int}(T)$ is the time of HPE.

Proof. Let $t_{ub} \in T$ be the time of HUBE. Follows from definition 7, we have

$$\frac{\partial}{\partial t_s} X(t_s, c, g) < \frac{\partial}{\partial t_g} X(t_g, c, g) \, .$$

Note that t_g is a critical point in terms of first partial derivative with a positive first partial derivative which has the highest emission among such points. It implies $t_g \leq t_{ub}$. And t_s a critical point in terms of first partial derivative with a negative first partial derivative which has the highest emission among such points. It implies $t_{ub} \leq t_s$. In other words, we have

$$t_g \leq t_{ub} \leq t_s \, .$$

On the other hand $\frac{\partial}{\partial t} X(t, c, g)$ is continuous on $[t_g, t_s]$. And by intermediate value theorem (Rudin, 1964), there exists some $u \in [t_g, t_s]$ such that

$$\frac{\partial}{\partial u} X(u, c, g) = 0 \, .$$

Note that t_{ub} is the upper bound of the CEP, then it must be $t_{ub} = u$, since it must have zero first partial derivative as the CEP is increasing when approaching t_{ub} and is decreasing when leaving t_{ub}. Then by proposition 4, t_{ub} is the time of HPE, that is $t_{ub} = t_p$, since it has zero first partial derivative. And hence we have $t_g < t_p < t_s$, which proves the theorem. $\square$

The subsequent definition is pivotal periods (piviods). Informally, a pivotal period is defined as the period when a country reached an early stage of RGE or a transitional period when a country entered the late stage of RSE. In determining piviods, we will implement the notion of Lipschitz continuity (Searcóid, 2007), in particular, the notion of short map (Searcóid, 2007). Therefore, we will first present the formal definitions of Lipschitz continuity and short map as follows.

Definition 8 (Lipschitz Continuity). Suppose a function $f : \mathbb{R} \supset S \to \mathbb{R}$. Let $K > 0$. The function f is said to be K-Lipschitz continuous (Searcóid, 2007) if and only if

$$\forall x, y \in S : \; |f(x) - f(y)| \leq K|x - y| \, .$$

If f is K-Lipschitz continuous and $K = 1$, then f is referred to as a short map (Searcóid, 2007).

Informally, Lipschitz continuity tells us the bound of steepness of a function at a point. This property allows us to develop the formal notion to pinpoint the pivotal periods. The formal definition of pivotal periods is presented as follows.

Definition 9 (Pivotal Periods)**.** Suppose a country $c \in C$ and a GHG $g \in G$. Suppose a map $\nu : L^2(\lambda) \to L^2(\lambda)$ defined by

$$\forall f \in L^2(\lambda) \forall t \in T : \ \nu[f](t) = \frac{f(t) - \inf_{u \in T} f(u)}{\sup_{u \in T} f(u) - \inf_{u \in T} f(u)} \ .$$

Note that ν is a continuous map (André, 2020). Also,

$$\forall f \in L^2(\lambda) : \ \mathrm{image}(\nu[f]) = [0, 1]$$

holds. Suppose $\mathrm{id} \in L^2(\lambda)$ is an identity map, that is,

$$\forall t \in T : \ \mathrm{id}(t) = t \,.$$

Note that id is continuous and bijective. Suppose another map $\Phi : [0, 1] \to [0, 1]$ defined by

$$\Phi := \nu[X_{c,g}] \circ \nu[\mathrm{id}]^{-1} \,.$$

Follows from the continuity of ν, id and $X_{c,g}$ then Φ is also continuous (André, 2020). Let $t_{ub} \in T$ be the time of HUBE and let $\rho > 0$. Then we define as follows:

i. Suppose
$$u := \begin{cases} t_g & : \text{RGE exists and } t_g \text{ is the time of RGE} \\ t_{ub} & : \text{RGE does not exist} \end{cases} \,.$$

Let
$$S_i \subseteq (\nu[\mathrm{id}](\inf T), \nu[\mathrm{id}](u))$$

such that the restriction $\Phi|_{S_i} : S_i \to [0, 1]$ is a short map. If $S_i \neq \varnothing$, then $B_\rho(v_i)$ centred at a point $v_i \in T$ is referred to as the 2ρ-increasing pivotal period (2ρ-inpiviod) if and only if
$$v_i = \nu[\mathrm{id}]^{-1}(\sup S_i) \,.$$

ii. Suppose
$$u := \begin{cases} t_s & : \text{RSE exists and } t_s \text{ is the time of RSE} \\ t_{ub} & : \text{RSE does not exist} \end{cases} \,.$$

Let
$$S_d \subseteq (\nu[\mathrm{id}](u), \nu[\mathrm{id}](\sup T))$$

such that the restriction $\Phi|_{S_d} : S_d \to [0, 1]$ is a short map. If $S_d \neq \varnothing$, then $B_\rho(v_d)$ centred at a point $v_d \in T$ is referred to as the 2ρ-decreasing pivotal period (2ρ-depiviod) if and only if
$$v_d = \nu[\mathrm{id}]^{-1}(\inf S_d) \,.$$

An important proposition related to the piviods and short map which will help us develop the algorithm to identify piviods computationally is presented in the following proposition.

Proposition 5. Suppose a country $c \in C$ and a GHG $g \in G$. (i) Assume that the inpiviod exists for the corresponding CEP. Follows from definition 8 and part i of definition 9, an expression

$$\forall x, y \in S_i : \ x \neq y \ \implies \ \frac{|\Phi(x) - \Phi(y)|}{|x - y|} \leq 1$$

holds. (ii) Now assume that the depiviod exists for the corresponding CEP. Likewise, follows from definition 8 and part ii of definition 9, an expression

$$\forall x, y \in S_d : \ x \neq y \ \implies \ \frac{|\Phi(x) - \Phi(y)|}{|x - y|} \leq 1$$

holds.

Some property related to HUBE, RGE, RSE and piviods is presented in the following proposition.

Proposition 6. Suppose a country $c \in C$ and a GHG $g \in G$. Suppose both inpiviod and depiviod exist. Let $B_{\rho_i}(v_i)$ be the $2\rho_i$-inpiviod. Let $B_{\rho_s}(v_d)$ be the $2\rho_s$-depiviod. Follows from definition 9,

$$v_i < t_p < v_d$$

necessarily holds, where $t_p \in \text{int}(T)$ is the time of HPE. Since $X_{c,g}$ is continuous, then by intermediate value theorem (Rudin, 1964), existences of the time of RGE $t_g \in \text{int}(T)$ and the time of RSE $t_s \in \text{int}(T)$ are necessary. And hence

$$v_i < t_g < t_p < t_s < v_d$$

holds.

The notion of HUBE, HPE and piviods can be used to rigorously describe whether a country is currently growing GHE of a certain GHG. The following proposition will present this observation in a rigorous manner.

Proposition 7. Suppose a country $c \in C$ and a GHG $g \in G$. Some rigorous insights about the country c with the GHG g are presented as follows:

    i. The country c is referred to as g-historically growing (g-HG) if the corresponding CEP has not been equipped with HPE period, has only the inpiviod (without the depiviod), and $\max T$ is in the HUBE period.

    ii. The country c is referred to as g-post extreme growth (g-PEG) if the corresponding CEP already has the HPE period and has both the inpiviod and the depiviod.

The subsequent observation is the historical expected growth rate. This notion is a single real-valued indicator related to the growth of GHE. In this matter, we will turn to the real dataset (Gütschow and Pflüger, 2023) and use the DEP instead of the CEP to deliver the actual value. The definition is presented as follows.

Definition 10 (Historical Expected Growth Rate). Suppose a map $\Delta : L^2(P_\alpha) \to L^2(P_\alpha)$ defined by

$$\forall f \in L^2(P_\alpha) \forall t \in \tilde{T} : \ \Delta[f](t) := \begin{cases} f(t+1) - f(t) & : t < \max \tilde{T} \\ 0 & : t = \max \tilde{T} \end{cases} .$$

Note that by theorem 1, we have

$$\forall f \in L^2(P_\alpha) : \ \Delta[f] \in L^2(P_\alpha).$$

The historical expected growth rate (HEGR) is a map $\text{HEGR} : L^2(P_\alpha) \to \mathbb{R}$ defined by

$$\forall f \in L^2(P_\alpha) : \ \text{HEGR}(f) := \text{E}\left[\Delta[f] \ \middle| \ \tilde{T} \setminus \{\max \tilde{T}\}\right],$$

where $\text{E}[\ \cdot \ | \ \cdot \ ] : L^1(P_\lambda) \times \tilde{\mathcal{A}} \to \mathbb{R}$ is conditional expectation operator (Brémaud, 2020).

Note that we define HEGR as a general operator on $L^2(P_\alpha)$ in definition 10. In fact, its true purpose will be applied to the DEP. A computable equivalent expression of HEGR is presented in the following theorem.

Theorem 7. *The expression*

$$\forall f \in L^2(P_\alpha) : \ \text{HEGR}(f) = \frac{1}{\alpha(\tilde{T}) - 1}\left(f(\max \tilde{T}) - f(\min \tilde{T})\right)$$

holds.

Proof. Let the map

$$\tilde{\mathcal{A}} \times \tilde{\mathcal{A}} \to [0, 1]$$
$$(A, B) \mapsto P_\alpha(B \mid A) =: P_{\alpha, A}(B)$$

denote the conditional probability with respect to the probability space $(\tilde{T}, \tilde{\mathcal{A}}, P_\alpha)$. Note that

$$\forall A, B \in \tilde{\mathcal{A}}: \ B \subseteq A \implies P_{\alpha, A}(B) = P_\alpha(B \mid A) = \frac{P_\alpha(B \cap A)}{P_\alpha(A)} = \frac{P_\alpha(B)}{P_\alpha(A)}$$

holds (Brémaud, 2020). Let $f \in L^2(P_\alpha)$. Follows from the property of Lebesgue integral (Salamon, 2016), the definition of conditional expectation as a Lebesgue integral (Brémaud, 2020) and the Radon-Nikodým property of $(\tilde{T}, \tilde{\mathcal{A}}, P_\alpha)$, we obtain

$$\begin{aligned}
\text{HEGR}(f) &= \text{E}\left[\Delta[f] \,\middle|\, \tilde{T} \setminus \{\max \tilde{T}\}\right] \\
&= \int_{\tilde{T} \setminus \{\max \tilde{T}\}} \Delta[f] \, \mathrm{d}P_{\alpha, \tilde{T} \setminus \{\max \tilde{T}\}} \\
&= \frac{1}{P_\alpha(\tilde{T} \setminus \{\max \tilde{T}\})} \int_{\tilde{T} \setminus \{\max \tilde{T}\}} \Delta[f] \, \mathrm{d}P_\alpha \\
&= \frac{1}{P_\alpha(\tilde{T} \setminus \{\max \tilde{T}\})} \int_{\tilde{T} \setminus \{\max \tilde{T}\}} \Delta[f] \frac{\mathrm{d}P_\alpha}{\mathrm{d}\alpha} \, \mathrm{d}\alpha \\
&= \frac{\alpha(\tilde{T})}{\alpha(\tilde{T} \setminus \{\max \tilde{T}\})} \frac{1}{\alpha(\tilde{T})} \int_{\tilde{T} \setminus \{\max \tilde{T}\}} \Delta[f] \, \mathrm{d}\alpha \\
&= \frac{1}{\alpha(\tilde{T}) - \alpha(\{\max \tilde{T}\})} \sum_{t \in \tilde{T} \setminus \{\max \tilde{T}\}} \Delta[f](t) \\
&= \frac{1}{\alpha(\tilde{T}) - 1} \sum_{t \in \tilde{T} \setminus \{\max \tilde{T}\}} f(t+1) - f(t) \\
&= \frac{1}{\alpha(\tilde{T}) - 1} \left(f(\max \tilde{T}) - f(\min \tilde{T})\right)
\end{aligned}$$

which proves the theorem. $\square$

In addition to HEGR, it is always convenient to perform conditioning on HEGR. That is, we take a relative HEGR on some measurable subset of $\tilde{T}$. The corresponding definition is presented as follows.

Definition 11 (Conditonal HEGR). Conditional HEGR is a map $\text{HEGR}(\,\cdot \mid \cdot\,) : L^2(P_\alpha) \times \tilde{\mathcal{A}} \to \mathbb{R}$ defined by

$$\forall f \in L^2(P_\alpha) \forall A \in \tilde{\mathcal{A}}: \ \text{HEGR}(f \mid A) := \text{E}\left[\Delta[f] \,\middle|\, A \setminus \{\max \tilde{T}\}\right].$$

An important property related to conditional HEGR is presented in the following theorem.

Theorem 8. *Let $I \subset \tilde{T}$ be some interval of historical discrete time, that is,*

$$\forall x \in B_{1.5}(t): \ x \neq t \implies \tilde{d}(x, t) = 1,$$

for every $t \in I$. Then the conditional HEGR given I is presented by

$$\forall f \in L^2(P_\alpha): \ \text{HEGR}(f \mid I) = \frac{1}{\alpha(I) - 1} \left(f(\max I) - f(\min I)\right).$$

Proof. Note that $\tilde{T}$ is similar to I in the sense that $\tilde{T}$ is also a discrete interval. Then with precisely the same method to that of proving theorem 7, the expression

$$\forall f \in L^2(P_\alpha): \ \text{HEGR}(f \mid I) = \frac{1}{\alpha(I) - 1} \left(f(\max I) - f(\min I)\right)$$

will be obtained. $\square$

16

The final observation regarding the CEP will be the conditional historical bound space (CHBS), which is presented in the following definition.

Definition 12 (Conditional Historical Bound Space). Suppose a country $c \in C$ and a GHG $g \in G$. Then suppose a map $b : L^2(\lambda) \times \mathcal{A} \to \mathbb{R}$ which is defined by

$$\forall f \in L^2(\lambda) \forall A \in \mathcal{A} : \ b(f \mid A) := \max_{t \in A \cap \tilde{T}} |\tilde{X}_{c,g}(t) - f(t)|$$

We define as follows:

  i. Conditional lower bound transformation (CLBT) is a map $\text{CLBT} : L^2(\lambda) \times \mathcal{A} \to L^2(\lambda)$ defined by

$$\forall f \in L^2(\lambda) \forall A \in \mathcal{A} \forall t \in T : \ \text{CLBT}(f \mid A)(t) := f(t) - b(f \mid A).$$

  ii. Conditional upper bound transformation (CUBT) is a map $\text{CUBT} : L^2(\lambda) \times \mathcal{A} \to L^2(\lambda)$ defined by

$$\forall f \in L^2(\lambda) \forall A \in \mathcal{A} \forall t \in T : \ \text{CLBT}(f \mid A)(t) := f(t) + b(f \mid A).$$

  iii. Conditional historical bound space (CHBS) is a triple $(A, \text{CLBT}(X_{c,g} \mid A), \text{CUBT}(X_{c,g} \mid A))$, for any $A \in \mathcal{A}$.

  iv. Historical lower bound transformation (HLBT) is a map $\text{HLBT} : L^2(\lambda) \to L^2(\lambda)$ defined by

$$\forall f \in L^2(\lambda) : \ \text{HLBT}(f) := \text{CLBT}(f \mid T).$$

  v. Historical upper bound transformation (HUBT) is a map $\text{HUBT} : L^2(\lambda) \to L^2(\lambda)$ defined by

$$\forall f \in L^2(\lambda) : \ \text{HUBT}(f) := \text{CUBT}(f \mid T).$$

  vi. Historical bound space (HBS) is a triple $(T, \text{HLBT}(X_{c,g}), \text{HUBT}(X_{c,g}))$.

A natural consequence on the CEP related to CHBS and HBS is presented in the following theorem.

Theorem 9. *Suppose a country $c \in C$ and a GHG $g \in G$. Suppose a CHBS $(A, \text{CLBT}(X_{c,g} \mid A), \text{CUBT}(X_{c,g} \mid A))$ and HSB $(T, \text{HLBT}(X_{c,g}), \text{HUBT}(X_{c,g}))$. The following statements hold:*

  i. $\forall t \in A : \ \text{CLBT}(X_{c,g} \mid A)(t) \leq X_{c,g}(t) \leq \text{CUBT}(X_{c,g} \mid A)(t)$

  ii. $\forall t \in T : \ \text{HLBT}(X_{c,g})(t) \leq X_{c,g}(t) \leq \text{HUBT}(X_{c,g})(t)$

Proof. We first prove statement i. Follows from definition 12, we have that

$$\text{image}(b) \subset [0, \infty) \,,$$

showing that

$$b(A) \geq 0 \,.$$

Then by part i and part ii of definition 12, we obtain

$$\text{CLBT}(X_{c,g} \mid A)(t) = X_{c,g}(t) - b(A) \leq X_{c,g}(t) \leq X_{c,g}(t) + b(A) = \text{CUBT}(X_{c,g} \mid A)(t) \,,$$

which proves statement i. Now we prove statement ii. Follows from the definitions of HLBT and HUBT in definition 12 part iv and part v as well as statement i earlier, we obtain

$$\text{HLBT}(X_{c,g})(t) = \text{CLBT}(X_{c,g} \mid T)(t) \leq X_{c,g}(t) \leq \text{CUBT}(X_{c,g} \mid T)(t) = \text{HUBT}(X_{c,g})(t)$$

for every $t \in T$. Hence statement ii is proven. □

With definitions, theorems and propositions related to HUBE, HPE, RGE, RSE, piviods, HEGR and CHBS presented in this subsection, we will investigate these properties on the dataset of the historical GHE (Gütschow and Pflüger, 2023). In the subsequent section, we will describe the algorithms built from this theory as well as its computational implementation in Python.

3.5 Algorithms for Computing CEP and Its Properties

In practice, we use Python to compute the rigorous properties of CEPs including HUBE, HPE, RGE, RSE, piviods, CLBT and CUBT. All these properties are represented as instance methods bundled in a Python class. We leverage the numerical and symbolic computational power by implementing Numpy (Harris et al., 2020) and SymPy (Meurer et al., 2017). In this section, we will present the algorithms for these rigorous properties of CEPs. Notable considerations are presented as follows:

  i. In equation 7, we use a Bernstein polynomial to generate a CEP. However, the unknown constants need to be determined. We use `LinearRegression` from Scikit-Learn (Pedregosa et al., 2011) to determine these unknown constants.

  ii. In computing critical points, such as when searching the time of HUBE, the time of RGE, the time of RSE, if we use analytic approach we need to compute differential equations (e. g., computing $\frac{\partial}{\partial t} X(t, c, g) = 0$ for the time of HUBE, $\frac{\partial^2}{\partial t^2} X(t, c, g) = 0$ for both the times of RGE and RSE). One way we can perform in an analytic approach is by using a computer algebra system (CAS) library in Python such as SymPy (Meurer et al., 2017). However, there is a huge chance that we may end up with a computational catastrophe and instabilities as the degree of CEP Bernstein polynomial gets very large. To avoid this possible issue, we use a numeric method instead for this case.

  iii. We will also use a numerical approach when computing the sets S_i and S_d in definition 9 for piviods.

The algorithms for the rigorous properties are presented as the following pseudocodes.

Algorithm 1 CEP

Require: GHE dataset of $c \in C$ and $g \in G$ containing $\tilde{T}$ and $\tilde{X}_{c,g}$; $n \in \mathbb{N}$, $w > 0$
Ensure: $X_{c,g}$
1: ML $\leftarrow$ `LinearRegression(fit_intercept= False)`   ▷ (Pedregosa et al., 2011)
2: $\varepsilon \leftarrow \max_{t \in \tilde{T}} \tilde{X}_{c,g}$ ▷ Setting ε with a huge number
3: $k \leftarrow 1$
4: **while** $k \leq n$ **do**
5:     $B \leftarrow \left(t \mapsto \{x \in \tilde{T} \mid t - w < x < t + w \right)$
6:     $y \leftarrow \left(t \mapsto \frac{1}{|B(t)|} \sum_{u \in B(t)} \tilde{X}_{c,g}(u) \right)$ ▷ Implementation of map MA in postulate 2
7:     **for all** $i \in \{0, 1, \ldots, k\}$ **do**
8:         $X_i \leftarrow \binom{n}{i} t^i (1-t)^{k-i}$
9:     **end for**
10:    Train ML on $((X_0, X_1, \ldots, X_k), y)$
11:    $\hat{y} \leftarrow \text{ML}(X_0, X_1, \ldots, X_k)$
12:    **if** $\varepsilon > \|y - \hat{y}\|_{2:y-\text{E}[y]}$ **then**
13:        $\varepsilon \leftarrow \|y - \hat{y}\|_{2:y-\text{E}[y]}$
14:        $p \leftarrow k$
15:    **end if**
16: **end while**
17: Train ML on $((X_0, X_1, \ldots, X_p), y)$
18: $(\beta_{c,g,0}, \beta_{c,g,1}, \ldots, \beta_{c,g,p}) \leftarrow$ regression coefficients
19: $X_{c,g} \leftarrow \left(t \mapsto \sum_{k=0}^{p} \binom{p}{k} \beta_{c,g,k} t^k (1-t)^{p-k} \right)$

Algorithm 2 HUBE

Require: $\tilde{T}$, $X_{c,g}$, $\rho > 0$, $\delta > 0$ ▷ δ shall be sufficiently small, e. g., $\delta \leftarrow 0.1$

Ensure: t_{ub}, $B_\rho(t_{ub})$ ▷ Definition 5

 1: $T \leftarrow [\min \tilde{T}, \max \tilde{T}]$ ▷ Compute with CAS

 2: $t_0 \leftarrow \min \tilde{T}$

 3: $t_1 \leftarrow \max \tilde{T}$

 4: $t \leftarrow t_0$

 5: $t_{ub} \leftarrow t_0$

 6: **while** $t \leq t_1$ **do**

 7:    **if** $X_{c,g}(t) > X_{c,g}(t_{ub})$ **then**

 8:      $t_{ub} \leftarrow t$

 9:    **end if**

10:    **if** $t + \delta > t_1$ **then**

11:      $t \leftarrow t_1$

12:    **else**

13:      $t \leftarrow t + \delta$

14:    **end if**

15: **end while**

16: $B_\rho(t_{ub}) \leftarrow (t_{ub} - \rho, t_{ub} + \rho) \cap T$ ▷ Compute with CAS

Algorithm 3 HPE

Require: $\tilde{T}$, $X_{c,g}$, $\rho > 0$, $\delta > 0$

Ensure: t_p, $B_\rho(t_p)$

 1: $T \leftarrow [\min \tilde{T}, \max \tilde{T}]$ ▷ Compute with CAS

 2: $t_{ub} \leftarrow$ time of HUBE   ▷ Compute with algorithm 2

 3: **if** $t_{ub} \notin \{\min \tilde{T}, \max \tilde{T}\}$ **then**

 4:    $t_p \leftarrow t_{ub}$

 5:    $B_\rho(t_p) \leftarrow (t_p - \rho, t_p + \rho) \cap T$

 6: **else**

 7:    $t_p \leftarrow$ None

 8:    $B_\rho(t_p) \leftarrow \varnothing$

 9: **end if**

Algorithm 4 RGE

Require: $\tilde{T}$, $X_{c,g}$, $\rho > 0$, $\delta > 0$ ▷ δ shall be sufficiently small, e. g., $\delta \leftarrow 0.1$

Ensure: $t_g \in \mathrm{int}(T)$, $B_\rho(t_g)$

 1: $T \leftarrow [\min \tilde{T}, \max \tilde{T}]$ ▷ Compute with CAS

 2: $\hat{T} \leftarrow \{\min \tilde{T} + k\delta \mid k \in \mathbb{N} \wedge k\delta \leq \max \tilde{T} - \min \hat{T}\}$

 3: $X' \leftarrow \frac{\partial}{\partial t} X$ ▷ Compute with CAS

 4: $t_{ub} \leftarrow$ time of HUBE   ▷ Compute with algorithm 2

 5: $t_g \leftarrow$ None

 6: $t \leftarrow t_{ub} - \delta$

 7: **while** $t > \min \hat{T} \wedge t_g =$ None **do**

 8:    **if** $\forall x \in B_\rho(t) \cap \hat{T} : x \neq t \implies X'(x) < X'(t)$ **then**

 9:      $t_g \leftarrow t$

10:      $B_\rho(t_g) \leftarrow (t_g - \rho, t_g + \rho) \cap T$ ▷ Compute with CAS

11:    **end if**

12:    $t \leftarrow t - \delta$

13: **end while**

Algorithm 5 RSE

Require: $\tilde{T}$, $X_{c,g}$, $\rho > 0$, $\delta > 0$ ▷ δ shall be sufficiently small, e. g., $\delta \leftarrow 0.1$
Ensure: $t_s \in \text{int}(T)$, $B_\rho(t_s)$
  1: $T \leftarrow [\min \tilde{T}, \max \tilde{T}]$ ▷ Compute with CAS
  2: $\hat{T} \leftarrow \{\min \tilde{T} + k\delta \mid k \in \mathbb{N} \wedge k\delta \leq \max \tilde{T} - \min \hat{T}\}$
  3: $X' \leftarrow \frac{\partial}{\partial t} X$ ▷ Compute with CAS
  4: $t_{ub} \leftarrow$ time of HUBE   ▷ Compute with algorithm 2
  5: $t_s \leftarrow$ None
  6: $t \leftarrow t_{ub} + \delta$
  7: **while** $t < \max \tilde{T} \wedge t_s =$ None **do**
  8:     **if** $\forall x \in B_\rho(t) \cap \hat{T} : x \neq t \implies X'(x) > X'(t)$ **then**
  9:         $t_s \leftarrow t$
10:         $B_\rho(t_s) \leftarrow (t_s - \rho, t_s + \rho) \cap T$ ▷ Compute with CAS
11:     **end if**
12:     $t \leftarrow t + \delta$
13: **end while**

Algorithm 6 Piviods

Require: $\tilde{T}$, $X_{c,g}$, $\rho > 0$, $\delta_0 > 0$, $\delta > 0$ ▷ δ shall be sufficiently small, e. g., $\delta \leftarrow 0.001$
Ensure: $B_\rho(v_i)$, $B_\rho(v_d)$ ▷ Definition 9
  1: $\nu[\text{id}] \leftarrow \left(t \mapsto \frac{t - \min \tilde{T}}{\max \tilde{T} - \min \tilde{T}} \right)$
  2: $\nu[\text{id}]^{-1} \leftarrow \left(x \mapsto x(\max \tilde{T} - \min \tilde{T}) + \min \tilde{T} \right)$
  3: $T \leftarrow [\min \tilde{T}, \max \tilde{T}]$ ▷ Compute with CAS
  4: $\hat{T} \leftarrow \{\min \tilde{T} + k\delta_0 \mid k \in \mathbb{N} \wedge k\delta_0 \leq \max \tilde{T} - \min \hat{T}\}$
  5: $X_{\min} \leftarrow \min_{t \in \hat{T}} X(t, c, g)$
  6: $X_{\max} \leftarrow \max_{t \in \hat{T}} X(t, c, g)$
  7: $\nu[X] \leftarrow \left(t \mapsto \frac{X(t,c,g) - X_{\min}}{X_{\max} - X_{\min}} \right)$
  8: $\Phi \leftarrow \nu[X] \circ \nu[\text{id}]^{-1}$
  9: $t_{ub} \leftarrow$ time of HUBE   ▷ Compute with algorithm 2
10: $t_g \leftarrow$ time of RGE   ▷ Compute with algorithm 4
11: $t_s \leftarrow$ time of RSE   ▷ Compute with algorithm 5
12: **if** $B_\rho(t_g) \neq \varnothing$ **then**
13:     $u_i \leftarrow t_g$
14: **else**
15:     $u_i \leftarrow t_{ub}$
16: **end if**
17: **if** $B_\rho(t_s) \neq \varnothing$ **then**
18:     $u_d \leftarrow t_s$
19: **else**
20:     $u_d \leftarrow t_{ub}$
21: **end if**
22: $W \leftarrow \{w_0, w_1, \ldots, w_{\frac{1}{\delta}}\}$ such that $w_0 = 0, w_{\frac{1}{\delta}} = 1$ and
        $\forall k \in \{1, \ldots, \frac{1}{\delta}\} : \; w_k - w_{k-1} = \delta$
23: $j \leftarrow 1$
24: **while** $j \leq \frac{1}{\delta}$ **do**
25:     **if** $|\Phi(w_j) - \Phi(w_{j-1})||w_j - w_{j-1}|^{-1} \leq 1$ **then**   ▷ Follows from proposition 5
26:         **if** $\nu[\text{id}]^{-1}(w_j) < u_i$ **then**
27:             $v_i \leftarrow \nu[\text{id}]^{-1}(w_j)$
28:             $B_\rho(v_i) \leftarrow (v_i - \rho, v_i + \rho) \cap T$ ▷ Compute with CAS
29:         **end if**
30:     **end if**
31:     **if** $|\Phi(w_{\frac{1}{\delta}-j}) - \Phi(w_{\frac{1}{\delta}-j-1})||w_{\frac{1}{\delta}-j} - w_{\frac{1}{\delta}-j-1}|^{-1} \leq 1$ **then**   ▷ Follows from proposition 5
32:         **if** $u_d < \nu[\text{id}]^{-1}(w_{\frac{1}{\delta}-k})$ **then**
33:             $v_d \leftarrow \nu[\text{id}]^{-1}(w_{\frac{1}{\delta}-k})$
34:             $B_\rho(v_d) \leftarrow (v_d - \rho, v_d + \rho) \cap T$ ▷ Compute with CAS
35:         **end if**
36:     **end if**
37:     $j \leftarrow j + 1$
38: **end while**

Algorithm 7 HEGR

Require: $\tilde{T}$, $\tilde{X}_{c,g}$
Ensure: $\text{HEGR}(\tilde{X}_{c,g})$
1: $\text{HEGR}(\tilde{X}_{c,g}) \leftarrow (\alpha(\tilde{T}) - 1)^{-1}(\tilde{X}(\max T, c, g) - \tilde{X}(\min T, c, g))$ ▷ Follows from theorem 7

Algorithm 8 Conditional HEGR

Require: $\tilde{T}$, $\tilde{X}_{c,g}$, Discrete Interval $I \subseteq \tilde{T}$ ▷ Generate I with CAS
Ensure: $\text{HEGR}(\tilde{X}_{c,g} \mid I)$
1: $\text{HEGR}(\tilde{X}_{c,g} \mid I) \leftarrow (\alpha(I) - 1)^{-1}(\tilde{X}(\max I, c, g) - \tilde{X}(\min I, c, g))$ ▷ Follows from theorem 7

Algorithm 9 b-Transformer

Require: $\tilde{T}$, $\tilde{X}_{c,g}$, $f \in L^2(\lambda)$, $A \in \mathcal{A}$
Ensure: $b(f \mid A)$ ▷ Ref. definition 12
1: $b(f \mid A) \leftarrow 0$
2: **for all** $t \in \tilde{T} \cap A$ **do**
3:     **if** $b(f \mid A) < |\tilde{X}_{c,g}(t) - f(t)|$ **then**
4:         $b(f \mid A) \leftarrow |\tilde{X}_{c,g}(t) - f(t)|$
5:     **end if**
6: **end for**

Algorithm 10 CLBT

Require: $\tilde{T}$, $\tilde{X}_{c,g}$, $f \in L^2(\lambda)$, $A \in \mathcal{A}$
Ensure: $\text{CLBT}(f \mid A)$
1: $b(f \mid A) \leftarrow b$-Transformer ▷ Compute with algorithm 9
2: $\text{CLBT}(f \mid A) \leftarrow (t \mapsto f(t) - b(f \mid A))$ ▷ Follws from part i of definition 12

Algorithm 11 CUBT

Require: $\tilde{T}$, $\tilde{X}_{c,g}$, $f \in L^2(\lambda)$, $A \in \mathcal{A}$
Ensure: $\text{CLBT}(f \mid A)$
1: $b(f \mid A) \leftarrow b$-Transformer ▷ Compute with algorithm 9
2: $\text{CUBT}(f \mid A) \leftarrow (t \mapsto f(t) + b(f \mid A))$ ▷ Follws from part ii of definition 12

Algorithm 12 HLBT

Require: $\tilde{T}$, $\tilde{X}_{c,g}$, $f \in L^2(\lambda)$
Ensure: $\text{HLBT}(f)$
1: $T \leftarrow [\min \tilde{T}, \max \tilde{T}]$ ▷ Compute with CAS
2: $b(f \mid T) \leftarrow b$-Transformer ▷ Compute with algorithm 9
3: $\text{HLBT}(f) \leftarrow (t \mapsto f(t) - b(f \mid T))$ ▷ Follws from part iv of definition 12

Algorithm 13 HUBT

Require: $\tilde{T}$, $\tilde{X}_{c,g}$, $f \in L^2(\lambda)$
Ensure: $\text{HLBT}(f)$
1: $T \leftarrow [\min \tilde{T}, \max \tilde{T}]$ ▷ Compute with CAS
2: $b(f \mid T) \leftarrow b$-Transformer ▷ Compute with algorithm 9
3: $\text{HLBT}(f) \leftarrow (t \mapsto f(t) + b(f \mid T))$ ▷ Follws from part v of definition 12

4 Rigorous Insights of Historical GHG Emissions

The theory which has been developed in section 3 will be implemented for investigating insights of historical GHG emissions for top 3 emitting countries of each GHG type. The computational implementation of the theory is conducted using Python in IPython. The IPython file of the computation is hosted on a GitHub repository which can be accessed on (Purnawan, 2024).

The top 3 emitting countries and the corresponding GHG types as extracted from the historical GHE dataset (Gütschow and Pflüger, 2023) is presented in table 1. We will now investigate the HUBE, HPE, piviods, HEGR, the last decade HEGR, HLBT and HUBT of these countries with respect the GHG types.

Table 1: Top 3 countries by GHE

Top 3 CH_4	Top 3 CO_2	Top 3 NO_2	Top 3 NF_3	Top 3 SF_6
China	United States	United States	Japan	China
United States	China	China	United States	United States
India	Russia	Russia	China	Japan

4.1 Rigorous Insights of Top 3 CH_4 Emitters

The properties of the CEPs of top 3 CH_4 emitters are presented in table 2. While the rigorous insights including period of HUBE, period of HPE, inpiviod, depiviod, HEGR, and the last decade HEGR are presented in table 3. Note that we leave the decimal expressions in the year intervals of period of HUBE, period of HPE, invipiod and depiviod. Then the CEPs, the HLBTs and the HUBTs of these countries are illustrated in figure 2.

Table 2: Properties of CEPs of top 3 CH_4 emitters

Country	w of unit Years	Polynomial Degree
China	3.00	30
United States	3.00	30
India	3.00	30

Table 3: Rigorous Insights of top 3 CH_4 emitters

Country	10-Period of HUBE*	10-Period of HPE*	10-Inpiviod*	10-Depiviod*	HEGR (Tons/Yr/Yr)	Last 10 HEGR (Tons/Yr/Yr)
CHN	(2012.3, 2022]	(2012.3, 2022]	(1941.1, 1951.1)	$\sim$	180882.35	-120000.00
USA	(1979.2, 1989.2)	(1979.2, 1989.2)	(1931, 1941)	(1993.3, 2003.3)	95845.60	-130000.00
IND	(2017, 2022]	$\sim$	(1942.2, 1952.2)	$\sim$	52573.53	10000.00

*Interval of years in mathematical notation

As we can observe from the result that China has the period of HUBE in the past decade. As HPE exists, it suggests that the peak CH_4 emission has been attained. The pivotal period of growing CH_4 emission for China was during the early-1940s to the early-1950s as shown by the piviod. Note that the resulting piviod is consistent with the illustration in figure 2, as the graph of the CEP of China starts bending upward around 1940s to 1950s. There has not been the depiviod for China, suggesting that the CH_4 emission has not significantly decreased. While the HPE does exist, it is still difficult to say that the CH_4 emission starts decreasing. The existence of HPE at the end of the record can be possibly caused by some fluctuations of China's CH_4 emission.

For the United States, the periods of both HUBE and HPE had occured a few decades ago, during the late-1970s to the late-1980s. The pivotal period of growing CH_4 emission was during the early-1930s to the early-1940s as shown by the piviod, which is again consistent with the
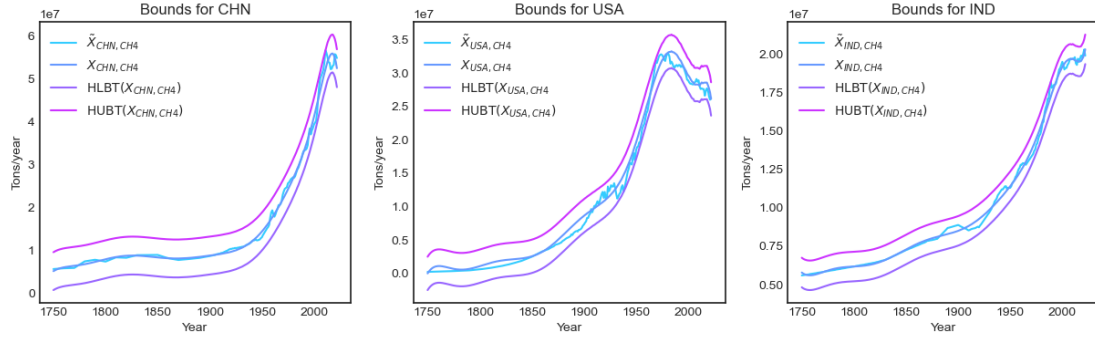
Figure 2: CEPs, HLBTs and HUBTs of top 3 CH_4 emitters

graph of the CEP of the United States in figure 2. The depiviod had existed during the early-1990s to the early-2000s. It is also evident from the graph that the United States has been entering the decreasing period of CH_4 emission, as also suggested by the negative value of the past decade HEGR. Thus, follows from proposition 7, the United States is a CH_4-PEG country.

For India, the period of HUBE was during 2017 to 2022, which was the recent time. While the HPE has not existed yet, suggesting that the CH_4 emission is expected to keep increasing. The pivotal period of growing CH_4 emission for India was during the early-1940s to the early-1950s as shown by the piviod, which is also consistent with the graph of the CEP of India. Follows from proposition 7, India is a CH_4-HG country as it has only inpiviod and the time of HUBE was at the latest record. The large value of the past decade HEGR also suggests the same conclusion.

4.2   Rigorous Insights of Top 3 CO_2 Emitters

The properties of the CEPs of top 3 CO_2 emitters are presented in table 4. While the rigorous insights including period of HUBE, period of HPE, inpiviod, depiviod, HEGR, and the last decade HEGR are presented in table 5. Then the CEPs, the HLBTs and the HUBTs of these countries are illustrated in figure 3.

Table 4: Properties of CEPs of top 3 CO_2 emitters

Country	w of unit Years	Polynomial Degree
United States	3.00	30
China	3.00	30
Russia	3.00	30

Table 5: Rigorous Insights of top 3 CO_2 emitters

Country	10-Period of HUBE*	10-Period of HPE*	10-Inpiviod*	10-Depiviod*	HEGR (Tons/Yr/Yr)	Last 10 HEGR (Tons/Yr/Yr)
USA	(1999, 2009)	(1999, 2009)	(1909.6, 1919.6)	$\sim$	1.87×10^7	-2.7×10^7
CHN	(2015, 2022]	(2015, 2022]	(1977.6, 1987.6)	$\sim$	4.25×10^7	1.80×10^8
RUS	(1979.2, 1989.2)	(1979.2, 1989.2)	(1933.5, 1943.5)	(1996.1, 2006.1)	5.88×10^6	-1.00×10^7

*Interval of years in mathematical notation

The period of HUBE of the United States with respect to CO_2 emisison was during the late-1990s to the late-2000s. Consequently, this period is also the HPE period since it was a few decades ago. The piviod of the United States was during the late 1900s to the late 1910s. Note that the resulting piviod is consistent with the graph of the CEP of the United States as illustrated in figure 3. There has not been the depiviod for the United States. However, the huge decrease of the past decade HEGR indicates the progress toward decreasing CO_2 emissions.
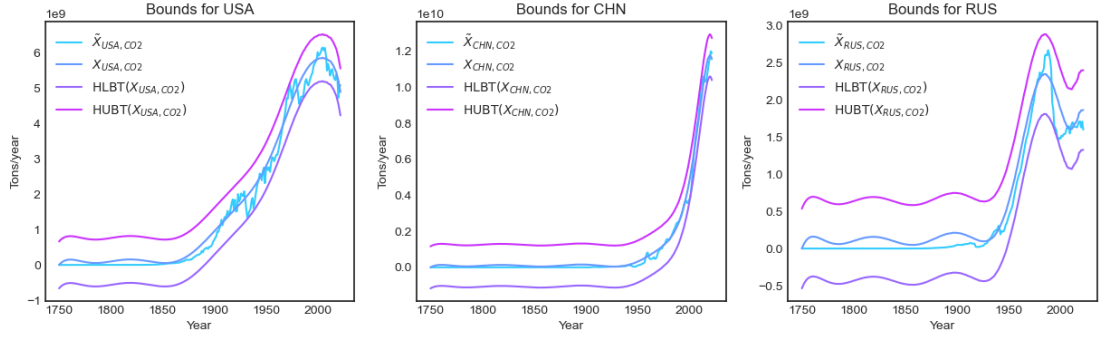
Figure 3: CEPs, HLBTs and HUBTs of top 3 CO_2 emitters

China is still entering the period of HUBE with respect to the CO_2 emission, which started from 2015. The computation shows that the HPE exists. However, it is still too early to settle the existence of HPE as changes may happen as the dataset (Gütschow and Pflüger, 2023) is updated. The pivoid of China was during the late-1970s to the late-1980s. This result is also consistent with the graph of the CEP of China as illustrated in figure 3. The depivoid has not existed. And China is still growing the CO_2 emission as confirmed by the huge value of the past decade HEGR which is roughly 4-times the value of the HEGR.

For Russia, the periods of HUBE as well as HPE were during the late-1970s to the late-1980s which was around the last decade of the Soviet era. The inpivoid of Russia was during the early-1930s to the early-1940s, which is consistent with the graph of the CEP of Russia in figure 3. The depivoid existed which happeed during the mid-1990s to the mid-2000s. Follows from proposition 7, Russia is a CO_2-PEG country as it has the HPE, and both the inpivoid and the depivoid. It is also consistent with the huge negative value of the past decade HEGR.

4.3 Rigorous Insights of Top 3 N_2O Emitters

The properties of the CEPs of top 3 N_2O emitters are presented in table 6. While the rigorous insights including period of HUBE, period of HPE, inpivoid, depivoid, HEGR, and the last decade HEGR are presented in table 7. Then the CEPs, the HLBTs and the HUBTs of these countries are illustrated in figure 4.

Table 6: Properties of CEPs of top 3 N_2O emitters

Country	w of unit Years	Polynomial Degree
United States	3.00	30
China	3.00	30
Russia	3.00	30

Table 7: Rigorous Insights of top 3 N_2O emitters

Country	10-Period of HUBE*	10-Period of HPE*	10-Inpivoid*	10-Depivoid*	HEGR (Tons/Yr/Yr)	Last 10 HEGR (Tons/Yr/Yr)
USA	(1978.7, 1988.7)	(1978.7, 1988.7)	(1926.2, 1936.2)	(1989.5, 1999.5)	5804.41	4000.00
CHN	(2013.6, 2022]	(2013.6, 2022]	(1948.7, 1958.7)	$\sim$	8139.41	5000.00
RUS	(1977, 1987)	(1977, 1987)	(1935.1, 1945.1)	(1999.6, 2009.6)	1017.65	4600.00

*Interval of years in mathematical notation

For the United States, the periods of HUBE as well as HPE with respect to the N_2O emission were during the late-1970s to the late-1980s. The pivoid was during the mid-1920s to the mid-1930s, which is consistent with the graph of the CEP in figure 4. The depivoid also existed
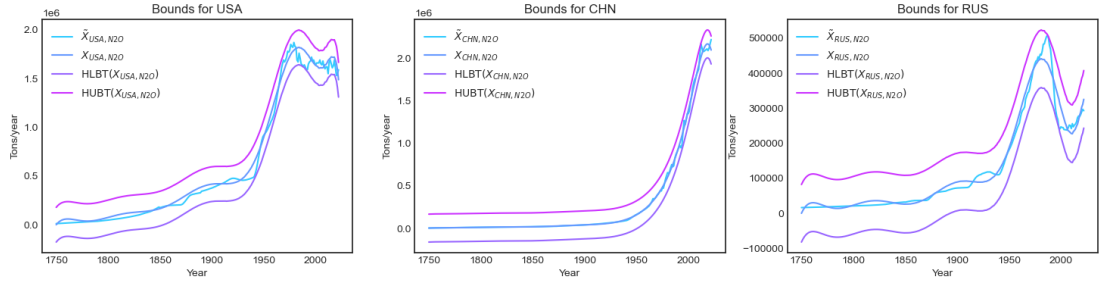
Figure 4: CEPs, HLBTs and HUBTs of top 3 N_2O emitters

which was during the late 1980s to the late 1990s. The recent times saw a fluctuational period for the United States, as indicated by the positive value of the pas decade HEGR, while on the other hand the country already has the depiviod. Follows from proposition 7, the United States is N_2O-PEG country.

The N_2O emission for China has a similar circumstance with the country's CH_4 and CO_2 emissions only with a different magnitude. The periods of HUBE as well as HPE were during the recent times, and the emission is still increasing as indicated by the past decade HEGR. The piviod for China was during the late-1940s to the late-1950s, which is consistent with the graph of the CEP in figure 4. The depiviod has not existed.

For Russia, the N_2O emission has a similar circumstance with the country's CO_2 emission, only with a different magnitude. The periods of HUBE and HPE of Russia with respect to the N_2O emission was during the late-1970s to the late-1980s. The piviod was during the mid-1930s to the mid-1940s, which is consistent with the graph of the CEP in figure 4. The depiviod existed, which was during the late 1990s to the late 2000s. In the recent times, the N_2O emission for Russia is relatively fluctuating toward increasing, as indicated by the positive value of the past decade HEGR. Follows from proposition 7, Russia is a N_2O-PEG country.

4.4 Rigorous Insights of Top 3 NF_3 Emitters

The properties of the CEPs of top 3 NF_3 emitters are presented in table 8. While the rigorous insights including period of HUBE, period of HPE, inpiviod, depiviod, HEGR, and the last decade HEGR are presented in table 9. Then the CEPs, the HLBTs and the HUBTs of these countries are illustrated in figure 5.

Table 8: Properties of CEPs of top 3 NF_3 emitters

Country	w of unit Years	Polynomial Degree
Japan	3.00	50
United States	3.00	50
China	3.00	50

Table 9: Rigorous Insights of top 3 NF_3 emitters

Country	10-Period of HUBE*	10-Period of HPE*	10-Inpiviod*	10-Depiviod*	HEGR (Tons/Yr/Yr)	Last 10 HEGR (Tons/Yr/Yr)
JPN	(2007, 2017)	(2007, 2017)	(1979.7, 1989.7)	∼	0.15	-4.76
USA	(2017, 2022]	∼	(1975.9, 1985.9)	∼	0.13	0.31
CHN	(2017, 2022]	∼	(1981.6, 1991.6)	∼	0.14	1.92

*Interval of years in mathematical notation

The periods of HUBE and HPE for Japan with respect to the NF_3 emission were during the mid-2000s to the mid-2010s. The inpiviod was during the early-1980s to the early-1990s, which
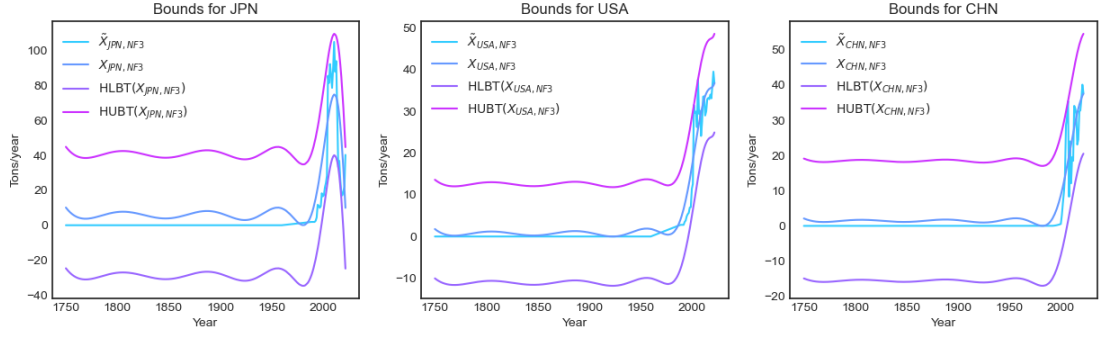
Figure 5: CEPs, HLBTs and HUBTs of top 3 NF$_3$ emitters

is consistent with the graph of the CEP in figure 5. The depiviod has not existed. However, Japan's NF$_3$ emission has been decreasing in the past decade as indicated by the negative value of the past decade HEGR.

For the United States, the periods of HUBE with respect to the NF$_3$ emission occurred during the recent times. The period of HPE has not existed, meaning that the NF$_3$ emission is still increasing. The inpiviod happed during the mid-1970s to the mid-1980s. The depiviod cannot occur, which is consistent with the absent of the HPE. The past decades HEGR indicates that the United States' NF$_3$ emission growth rate is roughly 2.5-times greater than the HEGR. And follows from proposition 7, the United States is a NF$_3$-HG country.

A similar case applies to China, with the period of HUBE with respect to the NF$_3$ emission was during the recent times. And the period of HPE has not existed either. The piviod of China was during the early-1980s to the early-1990s, which is consistent with the graph of the CEP in figure 5. The depiviod has not existed. China is relatively increasing the NF$_3$ emission, as indicated by the large value of the past decade HEGR which is roughly 14-times the value of HEGR. And follows from proposition 7, China is a NF$_3$-HG country.

4.5 Rigorous Insights of Top 3 SF$_6$ Emitters

The properties of the CEPs of top 3 SF$_6$ emitters are presented in table 10. While the rigorous insights including period of HUBE, period of HPE, inpiviod, depiviod, HEGR, and the last decade HEGR are presented in table 11. Then the CEPs, the HLBTs and the HUBTs of these countries are illustrated in figure 6.

Table 10: Properties of CEPs of top 3 SF$_6$ emitters

Country	w of unit Years	Polynomial Degree
China	3.00	50
United States	3.00	50
Japan	3.00	50

Table 11: Rigorous Insights of top 3 SF$_6$ emitters

Country	10-Period of HUBE*	10-Period of HPE*	10-Inpiviod*	10-Depiviod*	HEGR (Tons/Yr/Yr)	Last 10 HEGR (Tons/Yr/Yr)
CHN	(2017, 2022]	∼	(1993.6, 2003.6)	∼	15.55	323.00
USA	(1987.8, 1997.8)	(1987.8, 1997.8)	(1947.1, 1957.1)	(2009.7, 2019.7)	1.21	-2.50
JPN	(1987.4, 1997.4)	(1987.4, 1997.4)	(1949.5.5, 1959.5.5)	(2010.2, 2020.2)	0.33	-0.80

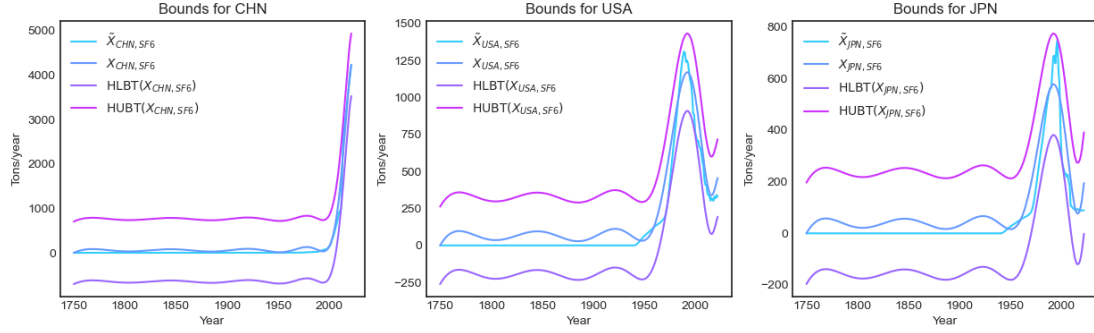*Interval of years in mathematical notation

Figure 6: CEPs, HLBTs and HUBTs of top 3 SF$_6$ emitters

China has the period of HUBE with respect to the SF$_6$ emission during the recent times. The HPE has not existed, giving a clear indication that the SF$_6$ emission is still growing. The piviod for China was during the early-1990s to the early-2000s. The depiviod has not existed. In the last decade, China increased a considerable amount of SF$_6$ emission, as indicated by the value of the past decade HEGR which is roughly 21-times the value HEGR. Follows from proposition 7, China is a SF$_6$-HG country.

The periods of both HUBE and HPE for the United States with respect to the SF$_6$ emission was during the late-1980s to the late 1990s. The inpiviod for the United States was during the late-1940s to the late-1950. The depiviod has existed for the United States, which was during the late-2000s to the late-2010s. Follows from proposition 7, the United States is a SF$_6$-PEG country. In addition, the United States' SF$_6$ emission significantly decrease in the past decades as indicated by the negative value of the past decade HEGR.

A similar circumstances happened for Japan. The periods of both HUBE and HPE for Japan with respect to the SF$_6$ emission was during the late-1980s to the late-1990s. The inpiviod was during the late-1940s to the late-1950s. The depiviod has existed which was during the early-2010s to the early-2020s. Follows from proposition 7, Japan is also a SF$_6$-PEG country. Japan's SF$_6$ emission also decreased in the past decade as indicated by the negative value of the past decade HEGR.

5   Conclusion and Future Works

We have demonstrated a rigorous and formal mathematical theory representing the historical GHG emissions as well as its properties in section 3. Rigorous and formal treatments allow us to designate novel concepts related the historical GHG emissions including HUBE, HPE, RGE, RSE, piviods (inpiviod and depiviod), HEGR, conditional HEGR and CHBS. We have also presented the algorithms for implementing the theory in the last subsection of section 3.

We have also conducted the computation for the analysis of the historical GHG emission by implementing this theory. The rigorous insights of this analysis have also been presented in section 4. It is evident that the theory, equipped with the versatility of formal mathematics, allows us to determine historical periods related to the GHG emissions according to the dataset (Gütschow and Pflüger, 2023) in an objective and unambiguous manner. A notable invention is the method for determining the piviods (pivotal periods) by leveraging the concept of Lipschitz continuity and short map (Searcóid, 2007).

An imperfection in this theory relates to the designation of the CEP using polynomial functions as it suffers from Runge's phenomenon (Runge, 1901). Runge's phenomenon is the oscillation at the edges of a domain interval of a function when approximated with a high degree polynomial (Runge, 1901). In section 4, we can see the CEPs of Russia in figures 3 and figure 4, Japan in figure 5, the United States and Japan again in figure 6 suffer from Runge's phenomenon at the edges of T. However, Bernstein polynomial (Lorentz, 2012) still offers a very good rep-

resentation that makes the Runge's phenomenon does not occur significantly and makes the representations still reliable. In fact, we experimented earlier by making use of ordinary polynomials and the effect of Runge's phenomenon was tremendous and the resulting representation was less accurate.

Another worth noting information is that the CEP requires a high degree Bernstein polynomial to make an accurate continuous representation for the DEP. In our case, the smallest degree is 30 and the largest degree is 50, which could be computationally expensive if the algorithms for the computation are not efficient. In our implementation, the performance is fair and is not quite expensive.

A point worth emphasizing is that the CEP generally cannot be used to accurately perform forecasting, since it is not the purpose of the CEP. The only purpose of the CEP in this paper is for representing the DEP as a differentiable function and only for historical analysis. In case one would use the CEP for a forecasting task, the CEP has to be properly treated further using a forecasting technique such as time series analysis (Ihaka, 2005).

The earlier point also implies that the rigorous insights presented in section 4 are temporary, meaning that these insights can change as the dataset (Gütschow and Pflüger, 2023) is updated in the future. In such a case, the properties of the CEP such as the polynomial degree, the unknown constants will also change based on the updated data and to obtain the new insights, the analysis shall be reiterated.

In future work, we aim to find an alternative designation of the CEP that avoids drawbacks like Runge's phenomenon for polynomials and is computationally efficient. Despite these challenges, our theory offers a novel method for analyzing historical GHG emissions, bridging the gap between formal mathematics and environmental science.

Acknowledgements

Funding

Declarations of Competing Interests

The author(s) declare that they have no known competing financial interests or personal relationships that could have appeared to influence the work reported in this paper.

Declaration of Generative AI and AI-Assisted Technologies in the Writing Process

During the preparation of this work, the author used ChatGPT to improve readability and language only in certain parts of the paper, namely the abstract, introduction, and conclusion. After using this tool/service, the author reviewed and edited the content as needed and takes full responsibility for the publication's content.

References

André, R. (2020). *Point-Set Topology with Topics*. Self-Published, Ontario.

Bergmann, M., Moor, J., and Nelson, J. (2014). *The Logic Book (Sixth Edition)*. McGraw-Hill, New York.

Brémaud, P. (2020). *Probability Theory and Stochastic Processes*. Springer, Cham, DOI: https://doi.org/10.1007/978-3-030-40183-2.

Dervos, C. T. and Vassilou, P. (2000). Sulfur hexafluoride (sf6): Global environmental effects and toxic byproduct formation. *Journal of the Air & Waste Management Association*, DOI: https://doi.org/10.1080/10473289.2000.10463996.

Gütschow, J. and Pflüger, M. (2023). The PRIMAP-hist national historical emissions time series (1750-2022) v2.5. DOI: 10.5281/zenodo.10006301, https://doi.org/10.5281/zenodo.10006301.

Gütschow, J., Jeffery, M. L., Gieseke, R., Gebel, R., Stevens, D., Krapp, M., and Rocha, M. (2016). The primap-hist national historical emissions time series. *Earth System Science Data*, 8:571–603, DOI: https://doi.org/10.5194/essd-8-571-2016.

Harris, C. R., Millman, K. J., van der Walt, S. J., Gommers, R., Virtanen, P., Cournapeau, D., Wieser, E., Taylor, J., Berg, S., Smith, N. J., Kern, R., Picus, M., Hoyer, S., van Kerkwijk, M. H., Brett, M., Haldane, A., del Río, J. F., Wiebe, M., Peterson, P., Gérard-Marchant, P., Sheppard, K., Reddy, T., Weckesser, W., Abbasi, H., Gohlke, C., and Oliphant, T. E. (2020). Array programming with NumPy. *Nature*, 585(7825):357–362, DOI: 10.1038/s41586-020-2649-2, https://doi.org/10.1038/s41586-020-2649-2.

Henderson, P. B. and Woytek, A. J. (2000). Fluorine compounds, inorganic, nitrogen. *Kirk-Othmer Encyclopedia of Chemical Technology*, DOI: https://doi.org/10.1002/0471238961.1409201808051404.a01.

Hunter, J. D. (2007). Matplotlib: A 2d graphics environment. *Computing in Science & Engineering*, 9(3):90–95, DOI: 10.1109/MCSE.2007.55.

Ihaka, R. (2005). *Time Series Analysis: Lecture Notes for 475.726*. Statistics Department, University of Auckland, https://www.stat.auckland.ac.nz/~ihaka/726/notes.pdf.

Kreyszig, E. (1978). *Introductory Functional Analysis with Applications*. Wiley, New York.

Lorentz, G. G. (2012). *Bernstein Polynomials: Second Edition*. American Mathematical Society.

Meurer, A., Smith, C. P., Paprocki, M., Čertík, O., Kirpichev, S. B., Rocklin, M., Kumar, A., Ivanov, S., Moore, J. K., Singh, S., Rathnayake, T., Vig, S., Granger, B. E., Muller, R. P., Bonazzi, F., Gupta, H., Vats, S., Johansson, F., Pedregosa, F., Curry, M. J., Terrel, A. R., Roučka, v., Saboo, A., Fernando, I., Kulal, S., Cimrman, R., and Scopatz, A. (2017). Sympy: symbolic computing in python. *PeerJ Computer Science*, 3:e103, ISSN: 2376-5992, DOI: 10.7717/peerj-cs.103, https://doi.org/10.7717/peerj-cs.103.

pandas development team, T. (2020). pandas-dev/pandas: Pandas. DOI: 10.5281/zenodo.3509134, https://doi.org/10.5281/zenodo.3509134.

Patel, S., Miao, J. H., Yetiskul, E., Anokhin, A., and Majmundar, S. H. (2022). *Physiology, Carbon Dioxide Retention*. StatPearls.

Pedregosa, F., Varoquaux, G., Gramfort, A., Michel, V., Thirion, B., Grisel, O., Blondel, M., Prettenhofer, P., Weiss, R., Dubourg, V., Vanderplas, J., Passos, A., Cournapeau, D., Brucher, M., Perrot, M., and Duchesnay, E. (2011). Scikit-learn: Machine learning in Python. *Journal of Machine Learning Research*, 12:2825–2830.

Purnawan, R. (2023). An exploration on a normed space called r-normed space: Some properties and an application. *MDPI preprints.org*, DOI: http://dx.doi.org/10.20944/preprints202310.1770.v1.

Purnawan, R. (2024). rizalpurnawan23/mathematical-representation-historical-ghg: Initial release (v0.1.0). DOI: https://doi.org/10.5281/zenodo.10695903.

Roman, S. (2005). *Advanced Linear Algebra (Second Edition)*. Springer, New York.

Rudin, W. (1964). *Principles of Mathematical Analysis*. McGraw-Hill, New York.

Runge, C. (1901). Über empirische funktionen und die interpolation zwischen äquidistanten ordinaten. *Zeitschrift für Mathematik und Physik*, 46:224–243.

Salamon, D. A. (2016). *Measure and Integration*. European Mathematical Society, Zurich.

Searcóid, M. O. (2007). *Metric Spaces: Lipschitz Functions*. Springer Verlag, London.

Sloss, L. L. (1992). *Nitrogen Oxides Control Technology Fact Book*. Noyes Data Corporation.

Stoll, R. R. (1963). *Set Theory and Logic*. Dover, New York.

Thiel, V. (2018). Methane carbon cycling in the past: Insights from hydrocarbon and lipid biomarkers. *Hydrocarbons, Oils and Lipids: Diversity, Origin, Chemistry and Fate*.

Treut, H. L., Somerville, R., Cubasch, U., Ding, Y., Mauritzen, C., Mokssit, A., Peterson, T., and Prather, M. (2007). Historical overview of climate change. In *Climate Change 2007: The Physical Science Basis*. Cambridge University Press, Cambridge, United Kingdom.